

AFRL-VS-HA-TR-98-0010

**DEVELOPMENT OF GENERALIZED
POLARIZATION ANALYSIS METHODS
FOR REGIONAL ARRAY DATA**

Zoltan A. Der

Robert H. Shumaway

**ENSCO, Inc.
5400 Port Royal Road
Springfield, VA 22151**

October 1997

Final Report

Approved for Public Release; distribution unlimited



**AIR FORCE RESEARCH LABORATORY
Space Vehicles Directorate
29 Randolph Road
AIR FORCE MATERIEL COMMAND
HANSCOM AFB, MA 01731-3010**

19990818 271

SPONSORED BY
Air Force Technical Applications Center
Directorate of Nuclear Treaty Monitoring
Project Authorization T/5101


MONITORED BY
Air Force Research Laboratory
CONTRACT No. F19628-95-C-0205

The views and conclusions contained in this document are those of the authors and should not be interpreted as representing the official policies, either express or implied, of the Air Force or U.S. Government.

This technical report has been reviewed and is approved for publication.



JAMES C. BATTIS
Contract Manager



CHARLES P. PIKE, Deputy Director
Integration and Operations Division

This report has been reviewed by the ESD Public Affairs Office (PA) and is releasable to the National Technical Information Service (NTIS).

Qualified requestors may obtain copies from the Defense Technical Information Center. All others should apply to the National Technical Information Service.

If your address has changed, or you wish to be removed from the mailing list, or if the addressee is no longer employed by your organization, please notify AFRL/VSOS-IM, 29 Randolph Road, Hanscom AFB, MA 01731-3010. This will assist us in maintaining a current mailing list.

Do not return copies of the report unless contractual obligations or notices on a specific document requires that it be returned.

REPORT DOCUMENTATION PAGE

Form Approved
OMB No. 0704-0188

Public reporting burden for this collection of information is estimated to average 1 hour per response, including the time for reviewing instructions, searching existing data sources, gathering and maintaining the data needed, and completing and reviewing the collection of information. Send comments regarding this burden estimate or any other aspect of this collection of information, including suggestions for reducing this burden, to Washington Headquarters Services, Directorate for Information Operations and Reports, 1215 Jefferson Davis Highway, Suite 1204, Arlington, VA 22202-4302, and to the Office of Management and Budget, Paperwork Reduction Project (0704-0188), Washington, DC 20503.

1. AGENCY USE ONLY (Leave blank)		2. REPORT DATE October 1997		3. REPORT TYPE AND DATES COVERED Final Report	
4. TITLE AND SUBTITLE Development of Generalized Polarization Analysis Methods for Regional Array Data				5. FUNDING NUMBERS F19628-95-C-0205 PE 35999F PR 5101 TA GM WU AK	
6. AUTHOR(S) Zoltan Der Robert Shumway					
7. PERFORMING ORGANIZATION NAME(S) AND ADDRESS(ES) ENSCO, INC. 5400 Port Royal Road Springfield, VA 22151				8. PERFORMING ORGANIZATION REPORT NUMBER	
9. SPONSORING/MONITORING AGENCY NAME(S) AND ADDRESS(ES) Air Force Research Laboratory 29 Randolph Road Hanscom AFB, MA 01731-3010 Contract Manager: James Battis/VSBI				10. SPONSORING/MONITORING AGENCY REPORT NUMBER AFRL-US-HA-TR-98-0010	
11. SUPPLEMENTARY NOTES Sponsored by Air Force Technical Applications Center Directorate of Nuclear Monitoring Issued by the Phillips Laboratory under Contract F19628-95-C-0205					
12a. DISTRIBUTION/AVAILABILITY STATEMENT Approved for Public Release; distribution unlimited				12b. DISTRIBUTION CODE	
13. ABSTRACT (Maximum 200 words) We are presenting test results on various non-conventional signal processing approaches as applied to data from regional seismic arrays. In particular, an adaptive approach for automatic identification of regional arrivals was tested. This method was designed to circumvent some difficulties that plagued previous attempts of 3-component polarization analyses for regional arrival identification. In particular, the methodology is designed to avoid complications due to signal distortion by near sensor geology and complex arrivals made up of superpositions of multiple independent signal components. The idea is to replace time delay operators and assumed particle motion patterns used in deterministic signal processing with empirically computed sets of transfer functions, using a learning set of relatively high S/N events. The application of this approach requires more than three sensor outputs (such as a 3-component combination plus some extra array sensors). We have tested both a frequency domain and a time domain approach to this algorithm. Thus far the frequency-domain version has reached a further stage of development. The methodology appears to be an attractive alternative to conventional array processing methods in quickly identifying and discriminating various arrivals from the same source region, or similar arrivals from different source regions at a small array. We are also addressing the problem of onset time estimation for regional arrivals. Most methods proposed thus far attempt to find the first point where the statistical properties of the seismic trace change. This is difficult or next to impossible with the often emergent regional arrivals. Instead, we are advocating a methodology based on the cumulative sum (CUSUM) of various statistics. Superposing a linear trend on the cumulative sum can make the changes in the trend of CUSUM to become minima of the resulting function. This function lends itself to the application of numerous algorithms for finding the minima of a function. Besides the viable method of onset time estimation by finding of absolute minima, repeated applications of simulated annealing (SA) results in populations of onset time estimates that can be treated with ordinary statistical methods. Tests of this methodology are very promising. CUSUM-based onset time estimation for Pn appears to be competitive to estimation of onset times by an analyst.					
14. SUBJECT TERMS seismology, array, signal processing, statistics, detection, identification, travel, time				15. NUMBER OF PAGES 86	
				16. PRICE CODE	
17. SECURITY CLASSIFICATION OF REPORT unclassified	18. SECURITY CLASSIFICATION OF THIS PAGE unclassified	19. SECURITY CLASSIFICATION OF ABSTRACT unclassified	20. LIMITATION OF ABSTRACT SAR		

TABLE OF CONTENTS

Abstract.....	iv
Objective.....	v
Organization of this Report	v
Analyses of the Generalized Polarization Processor	
Introduction	1
The Kola Peninsula Data Set.....	6
The Anatomy of Regional Arrivals	9
Outline of a Theoretical Framework for Regional Arrival Identification	
General Approach.....	15
Frequency Domain Approach	16
Time Domain Approach	18
Data Analysis	
Frequency Domain	20
Time Domain.....	40
Summary of Polarization Processing Results	
Phase Arrival Time Estimate at Regional Distances Using the CUSUM Algorithm	
Introduction	45
Combining CUSUM with Simulated Annealing	52
Evaluation of the Performance of the CUSUM Procedure for Estimating Pn Onset Times	55
Application of the CUSUM-SA Method to Segment Complete Regional Seismograms.....	62
Multichannel Deconvolution.....	71
Conclusions and Recommendations	
References	

Abstract

In this report we present test results on various non-conventional signal processing approaches as applied to data from regional seismic arrays. In particular, an adaptive approach for automatic identification of regional arrivals was tested to (*Der et al 1993*). This method was designed to circumvent some difficulties that plagued previous attempts of 3-component polarization analyses for regional arrival identification. In particular, the methodology is designed to avoid complications due to signal distortion by near sensor geology and complex arrivals made up of superpositions of multiple independent signal components. The idea is to replace time delay operators and assumed particle motion patterns used in deterministic signal processing with empirically computed sets of transfer functions using a learning set of relatively high S/N events. The application of this approach requires more than three sensor outputs (such as a 3-component combination plus some extra array sensors).

We have tested both a frequency domain and a time domain approach to this algorithm. Thus far the frequency-domain version has reached a further stage of development. The methodology appears to be an attractive alternative to conventional array processing methods in quickly identifying and discriminating various arrivals from the same source region, or similar arrivals from different source regions at a small array.

We are also addressing the problem of onset time estimation for regional arrivals. Most methods proposed thus far attempt to find the first point where the statistical properties of the seismic trace change. This is difficult or next to impossible with the often emergent regional arrivals. Instead, we are advocating a methodology based on the cumulative sum (CUSUM) of various statistics. Superposing a linear trend on the cumulative sum can make the changes in the trend of CUSUM to become minima of the resulting function. This function lends itself to the application of numerous algorithms for finding the minima of a function. Besides the viable method of onset time estimation by finding of the absolute minima, repeated applications of simulated annealing (SA) results in populations of onset time estimates that can be treated with ordinary statistical methods. Tests of this methodology are very promising. CUSUM-based onset time estimation for Pn appears to be competitive to estimation of onset times by an analyst.

Key Words: seismology, arrays, signal processing, statistics, detection, identification, travel time.

Objective

The objective of the work thus far is the facilitation of the automatic recognition of various regional arrivals. This is accomplished by a computational scheme for the adaptive learning of the generalized particle motion patterns as seen by small arrays that may also contain three-component sensors.

The purpose of the work is to relieve the human operator in seismic monitoring from the effort to identifying and locating routine blasting at various quarries and to enable him to possibly identify the sources of seismic waves from the Lg phase alone and to point out unusual events near some quarries that may merit further investigation. The techniques proposed do not have to be applied alone, but can be used jointly with other existing methods.

In the later part of this report we present results obtained by applying a new method that combines cumulative sums of a test statistic (CUSUM) and simulated annealing (SA), to solve the problem of automatic onset time estimation for regional seismic arrivals. Onset time estimation and segmentation of a regional seismogram into various kinds of seismic phase wave groups is part of an analyst's routine which appears to be amenable to automation.

Organization of this Report

This report consists of three parts. In the first part, we describe the testing of generalized polarization processor (*Der et al 1993*). In the second, we discuss the development of an onset time estimator based on CUSUM and SA. Finally, in the third part we describe work on other topics, in particular, modification made to the deconvolution program.

ANALYSES OF THE GENERALIZED POLARIZATION PROCESSOR

Introduction

Identification of regional "phases" at small seismic arrays, as currently practiced, is largely based on their slownesses and rectilinearity, frequency content and the time context they appear in on the seismograms. The concepts of slowness and rectilinearity implicitly imply the assumptions of plane waves and linear particle motion as models of seismic signals. Rectilinearity is based on simple halfspace models of P and S motion that have little relevance to the real world. Although these models fit many situations reasonably well, there are too many cases where such simple models fit the data only poorly. The issue is the quality of these fits. The question arises whether one could construct some more complex signal models that describe the spatial variations of waveforms better. Moreover, if such models can be found they may have considerable discriminative value in distinguishing the various arrival types at regional arrays. Assuming more complex multicomponent structure for regional waveforms has been shown to fit the actual motion better (*Der et al 1993*).

Slowness measurements across arrays are notoriously inaccurate because of the spatial variations of waveforms, which is incompatible with the plane wave propagation model. **Figure 1** is a good indication of what can be accomplished with these two measures using all elements of a regional array. It appears that slowness is still useful in separating P and S type (fast and slow) arrivals, while rectilinearity is of little value.

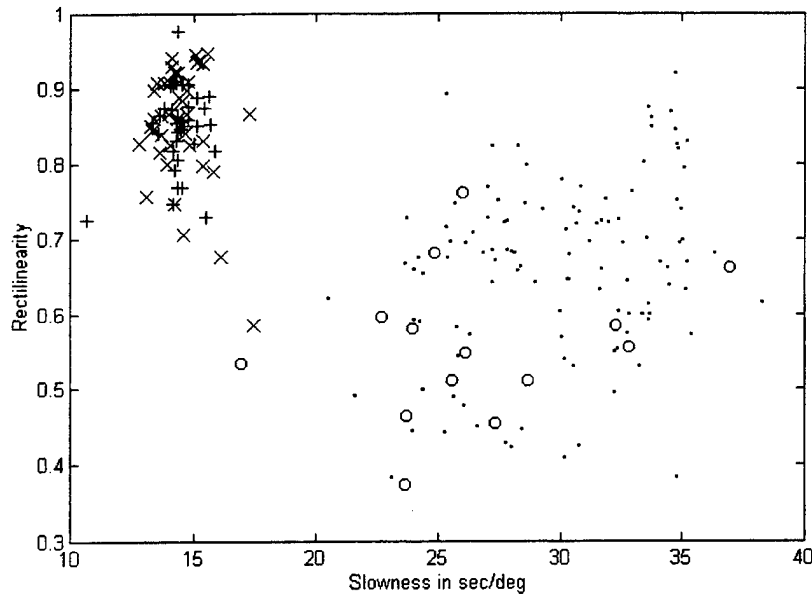


Figure 1. Plot of rectilinearity vs. slowness at ARCESS for various regional arrivals (plus signs for Pn, x for Pg, dot for Lg and circles for Sn) for a set of events recorded at ARCESS. The plot shows that while rectilinearity is of little value in distinguishing P and S type phases because of the large overlap, slowness separates them fairly well. Nevertheless P and S wave types constitute two mixed groups with no separation of Pn vs. Pg or Sn vs. Lg.

In earlier work (*Der et al 1993*), we have established the fact that the polarization patterns of regional arrivals, unlike simple P and/or S type motion patterns, cannot be fully described by three perpendicular components of motion. If this were the case, then it would be possible to derive one component of motion from the other two with some simple linear filters, but such was only possible for Pn, and not for the other regional arrivals. Moreover, we have found that two, rather than one, signal components are needed to model Pn. In general, in array processing one must have fewer independent signal components than the number of sensors in an array to make such waveform extrapolations possible. Sn and Lg seem to contain more signal components than two.

The particle motions of even supposedly simple 'P type' arrivals seem to be quite complex and three-dimensional. The situation is even more complex for other regional arrivals. Some of the complexities in the various regional arrivals can be explained by the fact that all regional arrivals are complex superpositions of multiple reflections in the crust and that each sensor location is also associated with some complex azimuth-slowness dependent transfer functions (often called site effects) that distort the waveform. The latter arise from geological complexi-

ties and topography near each sensor leading to waveform variations across even very small arrays.

Observations of regional waveforms at small arrays do not conform to the commonly used model of single plane waves propagating with uniform phase velocities either. If this were the case, then the waveforms of regional arrivals should be identical at all sensors of the same type and they are clearly not. Even if we are willing to include site-dependent simple site-transfer functions, then it should be possible to extrapolate the regional waveforms at one sensor from any of the other sensors. We have demonstrated (*Der et al 1993*) that this is not possible even for groups of events at nearly the same location.

These results are not unexpected, even in the conventional seismological framework. Regional arrivals can be described as complex superpositions of P and S waves multiply reflected in the crustal waveguide, (*Vogfford and Langston 1990*) or alternatively, higher modes of Love and Rayleigh type. As such they are not simple plane waves (since they are dispersive) and may have complex polarizations even for laterally homogeneous layered media. The three-dimensional heterogeneity of the Earth complicates the matter further, since this makes the 'site effects', i.e. intersite multichannel transfer functions, azimuth and slowness dependent.

The above statements should not be interpreted as declarations of the complete, dogmatic repudiation of conventional signal models, such as P and S wave models and plane waves. Obviously, they must have some validity, (*Christofferson and Roberts 1996*) since we are able to identify P motion about 50% of the time by polarization analysis; thus, with a high failure rate and F-K methods, based on the assumption of simple plane waves, still give valuable diagnostic information with regards to slowness and azimuth. We merely point out that these models do not describe the properties of the observed regional data well. Moreover, some gross features of the processing schemes we developed can also be explained in terms of processing for simpler models, but not in detail. If the simple polarization or plane wave models were exactly valid our processing schemes would simply reduce to some of the familiar simple processing schemes, such as beamforming.

In this report the term "polarization" describes the set of complex, frequency dependent transfer function relationships among the various sensors of a seismic array that may have any mix of

vertical and horizontal seismometers. The “polarization” changes as various types of seismic phases arrive and this will give us an opportunity to discriminate the various arrivals. In this sense, even an array containing only vertical sensors provides polarization information, even though most of the phase shifts may be associated with propagation delays. The observations mentioned lead to a type of generalized multichannel signal models for

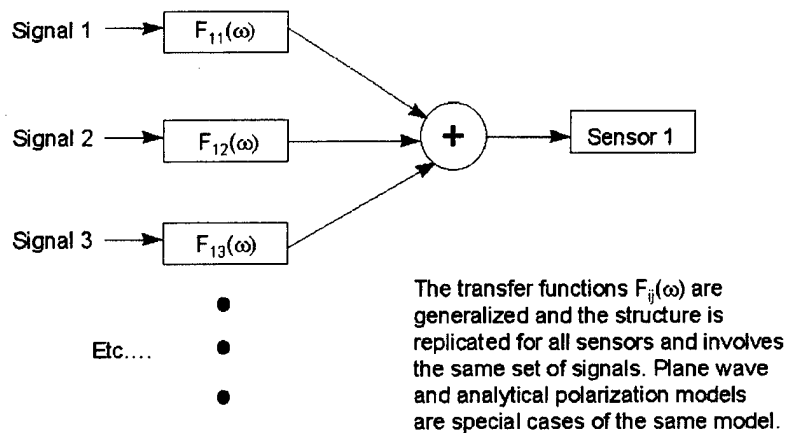


Figure 2. Generalized polarization model. Multiple independent signal processes are passed through generalized transfer functions to produce a sensor input. The whole structure each time involving different transfer functions but the same set of signal processes, is replicated as many times as there are sensors.

regional arrivals illustrated in **Figure 2** assuming that

- a) All of the regional arrivals contain more than the one or two independent (orthogonal) signal components assumed to be present in P and S type arrivals respectively.
- b) The waveforms of each sensor in a seismic array (including 3-component combinations) are to be regarded as outputs of such multiple signal components as passed through some sets of multichannel linear filters related to site-effects and various frequency-dependent propagation delays. Such multichannel filters will be assumed to remain constant for the same regional arrivals for events at the same distance and azimuth from the array.
- c) Multiple events at nearly the same locations, therefore, will be assumed to be independent replications that contain the same set of multichannel filters and thus can be used to build up statistics used in the detection and identification of various regional arrivals at that distance and azimuth.

Needless to say, some of these assumptions must be verified using data. While such assumptions are not useful for isolated single events, repeated events at nearly the same location are inevitable consequences of mining activity, and thus multiple events at nearly the same location are common. Thus, the basic idea underlying our approach is to replace time delay operators and assumed particle motion phase shifts used in deterministic signal processing (*Kwaerna and Ringdal 1992*) with empirically computed sets of transfer functions and a general multi-signal model. Although the plausibility of a multiple-signal multichannel model has been demonstrated for a limited sets of Kola peninsula events (*Der et al 1993*), much needs to be done to extend these finding to other set of events. In that paper it has been shown that Pn contained two signal components instead of one, and Sn and Lg must contain more. This was shown by semi-qualitative comparisons of multichannel predictions of one channel from the rest for a mini-array consisting of a three-component combination and a small tripartite vertical array. This work does not answer the following questions however:

- a) How many effective signal components are present in Sn and Lg?
- b) How do these things vary with distance and region and arrival?
- c) What statistical framework must be set up for detection and discrimination of the various regional arrivals?
- d) What is the best minimum sensor configuration to use?
- e) What is the most parsimonious model (both in terms of signal components and time domain filter coefficients) that is still effective?

One can arrive at an alternative way to look at the problem by considering the fact that a multisensor seismic array samples the motion at a small portion of a heterogeneous and possibly anisotropic elastic continuum at a few points. Clearly, since these points are elastically connected together they cannot move independently from each other. Nevertheless, there must be, intuitively, some ways to distinguish the generalized particle motion of the various arrivals as long as the source-to-array paths and compositions in terms of independent generalized signal

processes are similar. Conventional analytical particle motion and propagation models of wave types are of limited use here.

The Kola Peninsula Data Set

Throughout this report we present the results of data analyses performed on a data set of Kola peninsula quarry blasts as recorded at ARCESS. This was part of a data set that was assembled at ENSCO. All the events, quarry blasts, occurred during 1990. The quarry blasts were grouped into event sets with respect to their locations as determined by the IMS (*Bache and Bratt 1990*) and also considering their visible characteristics as originating in areas (quarries) named K1, K2, K3, K4, K5 and K8. There is no independent confirmation, “ground truth”, of the validity of these groupings, and they may be in error. In **Figure 3**, we show a scatter plot of their locations retrieved from their CMR origin files together with the location determined at ARCESS. These scatter plots show some outliers and overlaps of locations of events that were supposed to have taken place in the same quarry. Note that two events supposedly at mine K4 are grouped in location with the cluster of K1, K2 and K5 events. One of the K2 events is an outlier in this location plot. The K8 and the rest of the K4 events are clearly grouped at two distinct locations compared to the rest. The original association of these events with mines was based on waveform characteristics at the stations of the Finnish seismic network. A reevaluation of locations may be necessary including the ARCESS data. We had seven events at K1, nine at K2, eleven at K4, five at K5 and five at K8.

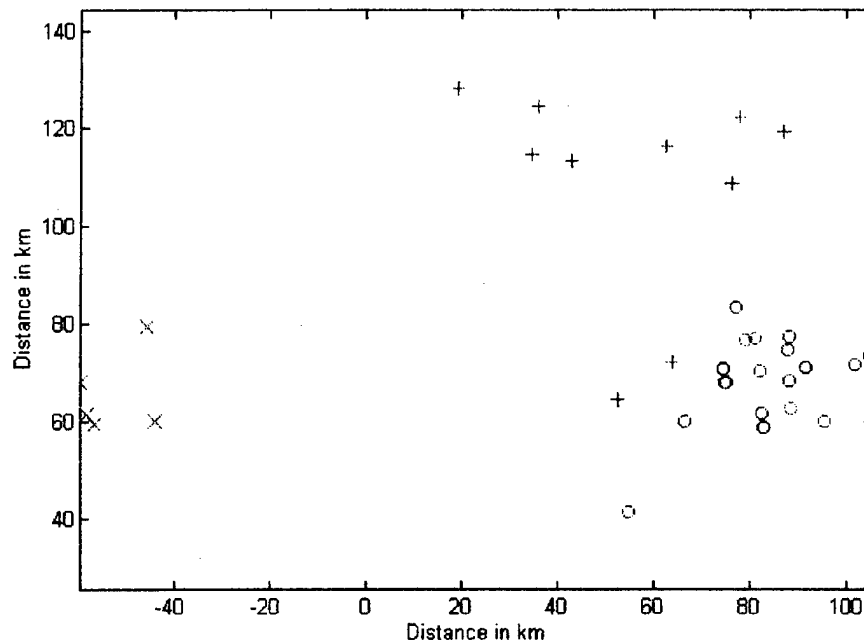


Figure 3. Scatter plot of the relative locations of Kola peninsula quarry blasts analyzed as reported by the IMS. The blue circles -- K2, red plus signs -- K4, red x letters --K8.

In this report we use only six-element arrays, subsets of ARCESS, in two major configurations, the “mini-array” used in *Der et al (1993)* which consists of a three-component combination at A0 combined with three vertical components in the C ring, and an “all vertical” array that combines the vertical component at A0 with two vertical components in the B ring and three in the C ring. The choice of this odd combination of sensors was not entirely free, but dictated by the commonality of error free traces among events and mines. We tried to maximize the amount of data common error free traces, available. In processing the data we extrapolate the trace A0 from the rest using a five-channel multichannel filter. Increasing the number of traces could increase the efficiency of the processes, provided that more events become available. Throughout the report the events are designated by letter-number combinations such as K2110, where the first two characters designate the mine K2, and the last three numbers the date of the event (in year 1990). Most of the events have high S/N ratios on the broad-band displays; thus, noise is not a major factor in our analyses. Table I contains the location information and local magnitudes of the events used for various data analyses in this report. As can be seen from the table the K4 mine magnitudes, as a whole, are lower than the magnitudes at the other mines. Therefore, the S/N ratios of these events are lower and thus are less suitable for designing filters.

TABLE I

Event	ML	Lat	Long
K1171	2.19	67.6315	33.8952
K1189	2.09	67.6110	33.7267
K1224	2.18	67.5642	34.0417
K1280	2.23	67.6881	33.8215
K1287	2.40	67.5388	34.1983
K1301	2.43	67.6908	33.8736
K2054	2.92	67.6448	34.3462
K2066	3.20	67.6148	34.0296
K2110	2.51	67.6098	33.7326
K2147	2.26	67.6951	34.0329
K2182	2.61	67.6695	34.0270
K2219	2.06	67.3717	33.2637
K2246	2.30	67.5401	33.5353
K2282	2.18	67.7470	33.7759
K2285	2.41	67.5525	33.9008
K4025	2.21	68.1233	32.8311
K4118	2.03	67.9800	33.7571
K4130	2.16	68.0203	32.9889
K4139	2.15	68.0327	32.7990
K4146	2.10	68.1001	33.7935
K4178	2.06	67.5819	33.2103
K4221	2.08	68.1549	32.4478
K4230	2.07	68.0483	33.4415
K4244	2.11	68.0751	33.9987
K4270	2.10	67.6490	33.4750
K5040	2.66	67.6357	33.7198
K5089	2.59	67.6388	34.1093
K5125	3.13	67.5261	33.9092
K5222	2.24	67.6576	34.4123
K5278	2.70	67.6390	34.4300
K8178	2.10	67.7142	30.9485
K8223	2.03	67.6126	30.6305
K8279	2.12	67.5405	30.9881
K8286	2.17	67.5346	30.7000
K8301	2.17	67.5552	30.6578

The Anatomy of Regional Arrivals

In order to optimize the processing of the data it is prudent to gain some understanding of the overall properties of the various arrivals from the various quarries as seen through some rather conventional analyses. A simple approach is to run data from some sensors through a bank of band-pass filters to assess frequency contents and relative amplitudes of each arrival. In this report we use the standard Pn-Pg-Sn-Lg-Rg designations with the full understanding that such may not be very meaningful in the physical sense. More careful analyses of regional seismograms made clear that Pg and Lg, for instance, are likely to be made up of complex superpositions of various wave types such as multiple reflections in the crust (*Vogfford and Langston 1990*).

We have run some representative events through band-pass filters. Most events from the K1 and K2 mines (including the K2 mine events analyzed in *Der et al 1993*) show indications of arrivals that can be tagged as Pn, Pg, Sn and Lg (**Figures 4 & 5**). The Pn, Pg and Sn arrivals are usually the most pronounced in the highest frequency bands, but Lg is the strongest in the 3-6 Hz range. At higher frequencies Lg is mixed up in the strong coda of the three earlier arriving phases. This makes the use of filters delimiting the Lg in the 3-6 Hz band advisable during processing of Lg.

The K4 mine events show relatively weak expressions of the phases Pg and Sn at ARCESS, but have a very strong Pn with a prolonged coda in the high frequency bands (**Figure 6**). The Pn arrival is often, but not always, emergent. The Lg phase is dominant in the 3-6 Hz band and, for some events, the Rg in the lower frequency bands. The K5 mine waveforms are again similar to those from K1 and K2 (**Figure 7**) with the Pn, Pg, Sn and Lg visible and distinct. The K8 mine events have two diffuse wavegroups, P and S types with no individual arrivals seen in either of them (**Figure 8**).

The waveform characteristics show clear correlation with the areal distribution of the events. Since the K1, K2 and K5 events are closely located, their waveform characteristics and frequency structures are similar. The K4 events are apparently distributed over a wide area, and may not be at the same quarry at all. The K8 events are much closer to ARCESS. The back-azimuths of the K8 and K4 events are also different from that of the K1-K2-K5 group.

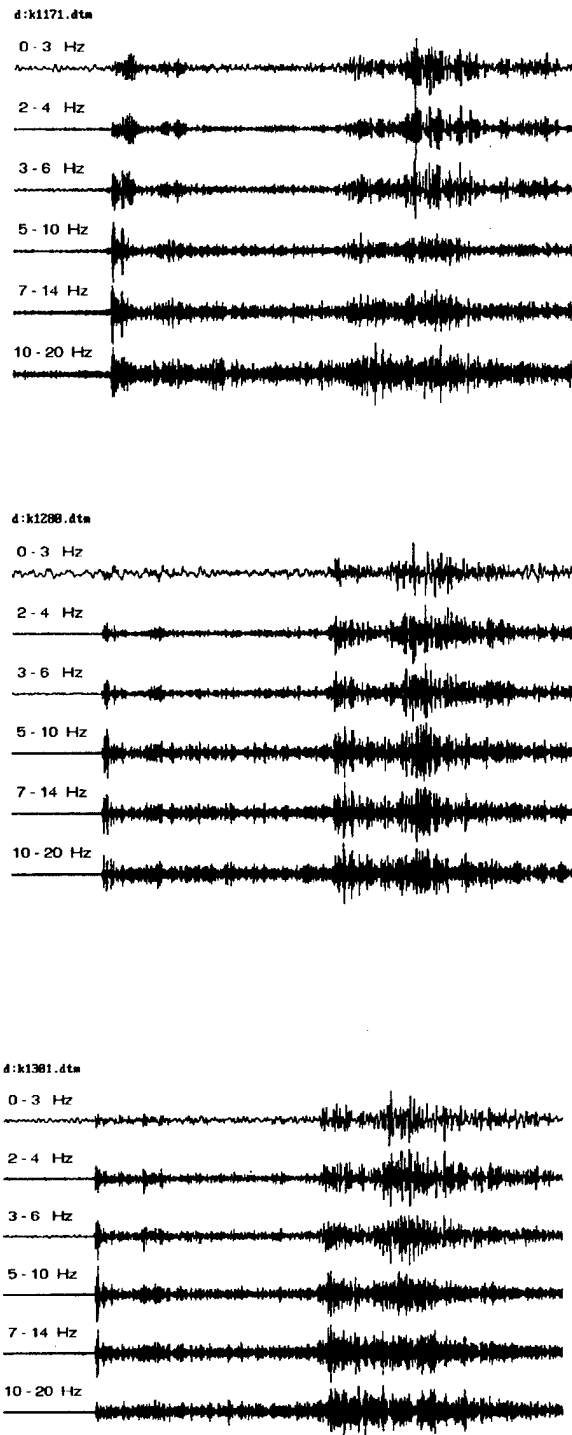


Figure 4. Band-pass filtered A0 seismograms for selected K1 mine events. The traces shown are 102 seconds long.

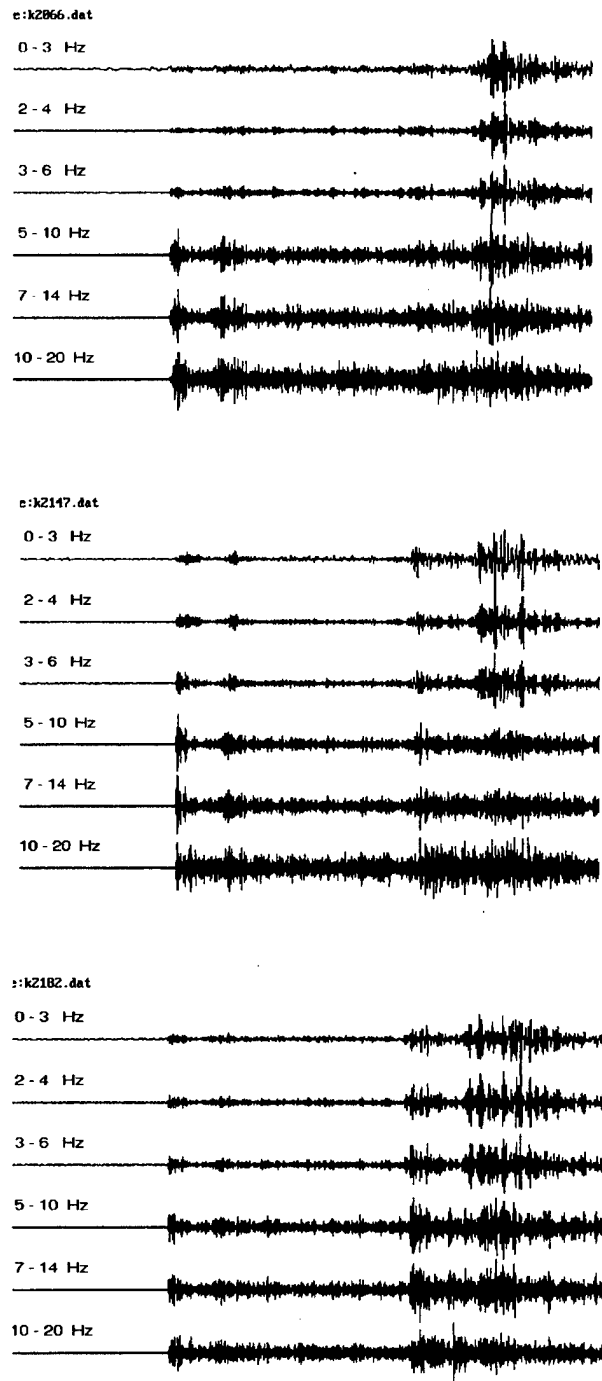


Figure 5. Band-pass filtered A0 seismograms for selected K2 mine events. The traces shown are 102 seconds long.

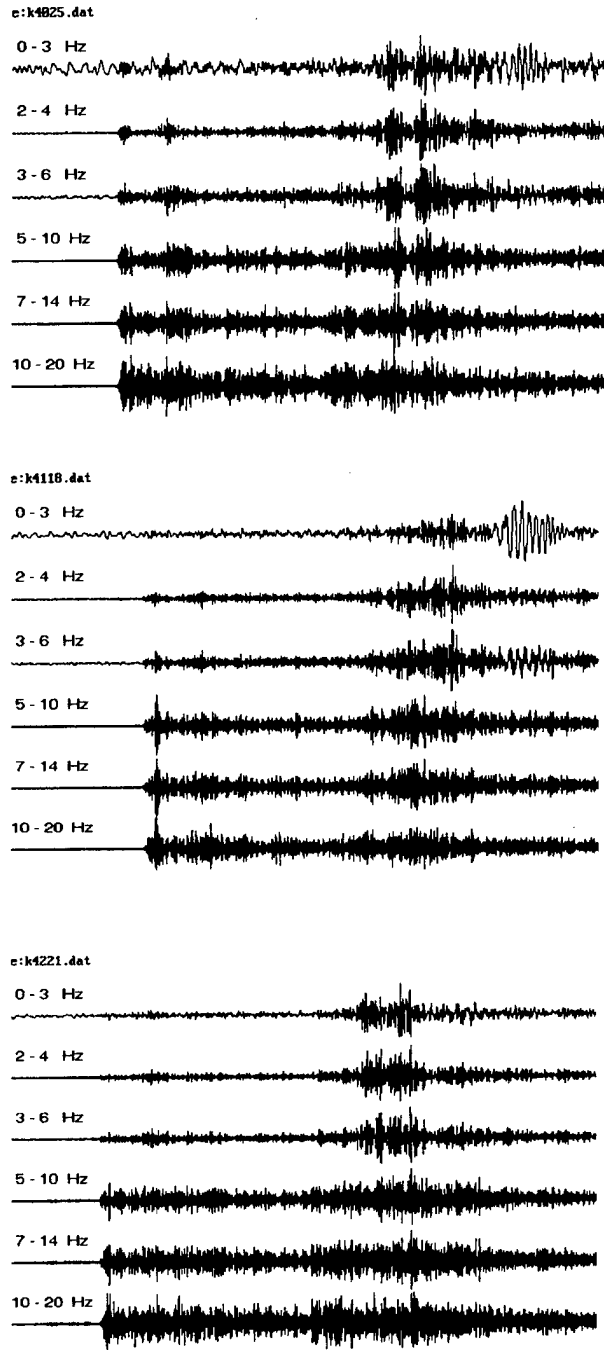


Figure 6. Band-pass filtered A0 seismograms for selected K4 mine events. The traces shown are 102 seconds long.

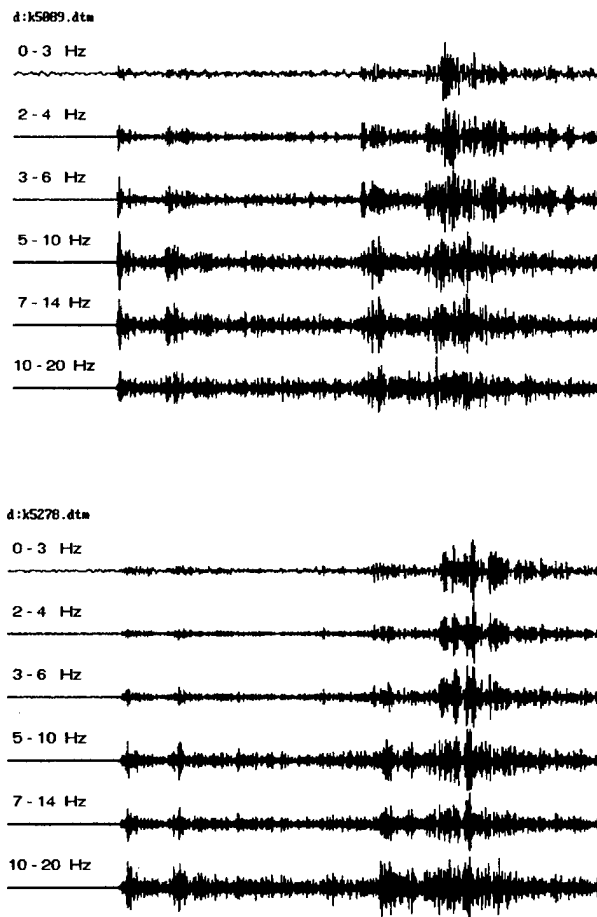


Figure 7. Band-pass filtered A0 seismograms for selected K5 mine events. The traces shown are 102 seconds long.

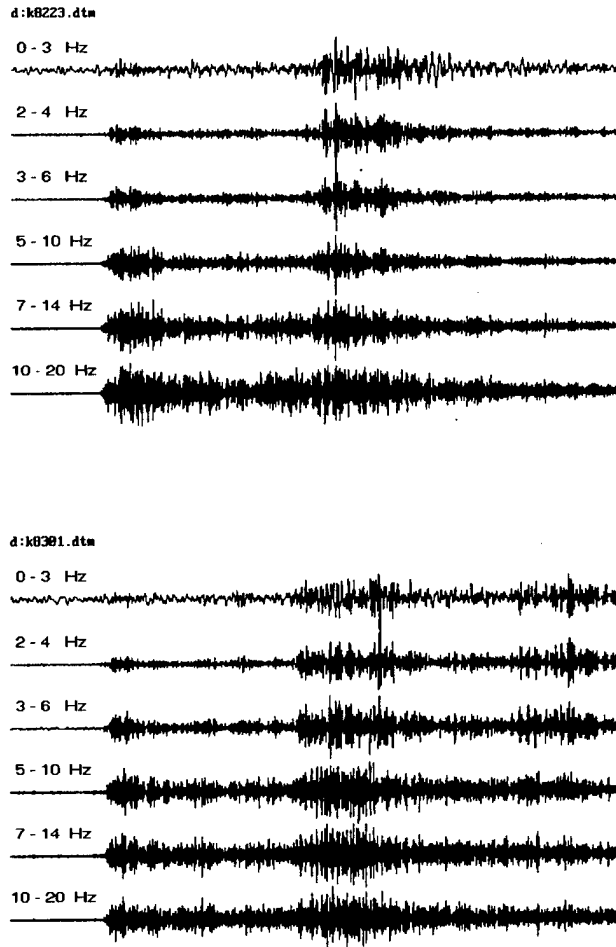


Figure 8. Band-pass filtered A0 seismograms for selected K8 mine events. The traces shown are 102 seconds long.

A common problem is the dominance of low frequencies in the noise, a common property of microseisms. Including these low frequencies in the processing initially caused high correlations for all filters designed to detect various phases in the noise windows preceding the events. When we limited the processing to frequencies above 1 Hz, where most of the signals dominate, this problem was remedied.

OUTLINE OF A THEORETICAL FRAMEWORK FOR REGIONAL ARRIVAL IDENTIFICATION

General Approach

Assuming that the multichannel structure of signals is as depicted in Figure 2, this would have the consequence that waveforms at any sensor could be reconstructed from the waveforms at the rest of the sensors as long as the number of independent signal processes is less than the number of the sensors of the array. The mode of reconstruction depends on the matrix of frequency-dependent transfer functions and not on detailed time histories of the individual processes. As long as the matrix of transfer functions is the same for a set of events, the reconstruction could be effectively accomplished using the same set of multichannel filters (Figure 9). When this matrix is different for an event (possibly because of a different modal composition, azimuth and slowness structure) a noticeable degradation should occur. The filter design and performance evaluation can be performed in both the time and frequency domains using cross-correlation function or spectral matrices constructed from a set of training events (quarry blasts) known to be at the same location. The formulas used for filter design are standard (*Shumway 1989, Wiggins and Robinson 1965*). The time domain performance evaluation uses the time domain RMS error and a likelihood ratio methodology, and the frequency domain approach uses the power residuals and F statistics.

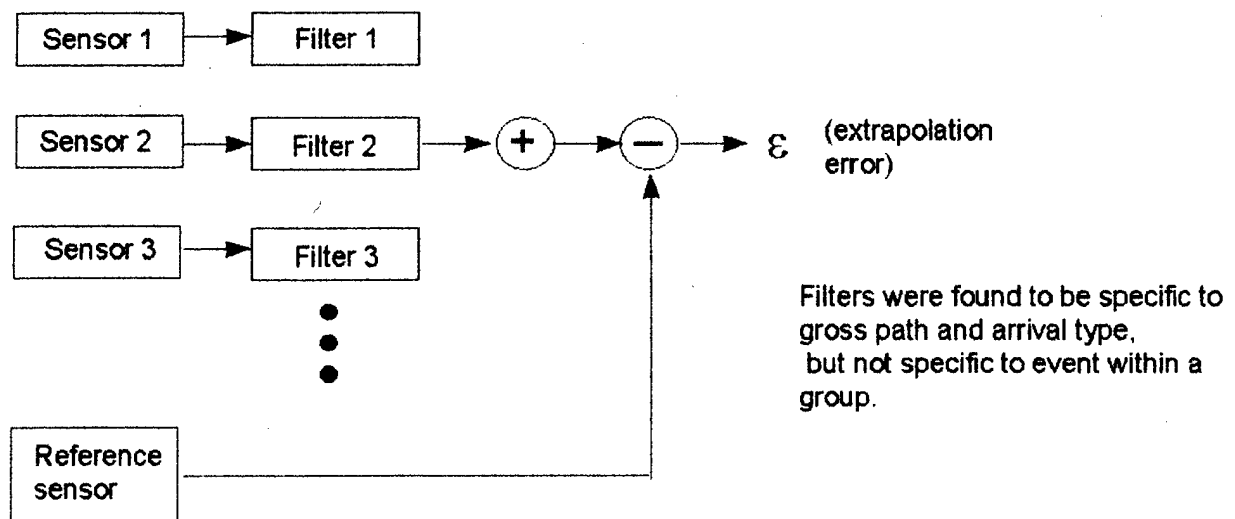


Figure 9. Processing flow of the small array polarization processor.

The time domain errors or power residuals should be small for events belonging to the same group as the training events, and large for the events not belonging to the group.

Frequency Domain Approach

Typically, there are a number of events at a given quarry which must be used to construct a spectral matrix of all the sensors by event compounding the cross products of the Fourier transforms of the time windows placed over the various arrivals seen in the seismogram.

It is desirable that the time windows are placed consistently, although small inaccuracies are of no consequence. Typically, we have lined up the Pn arrivals at the sensor A0 and placed the 256 point (6.4 second) windows preceding it by about 50 points. This way the first arrival was not tapered, but the window included some noise that was rather small for all events. The first and last 30 points of the windows were tapered off using a cosine taper. The windows for the later phases were placed at consistent time intervals relative to the Pn windows. The starting times of the Pg and Sn windows again preceded the visible arrival to avoid tapering the initial part of these arrivals. The Lg windows were placed on the initial large amplitude part of this phase since this part was shown to be more coherent across arrays (*Der et al 1986*). Propagation delays across the arrays were not considered in the placing the windows, i.e. the windows for all the sensors are time-aligned, since time delays are considered implicitly in the computed transfer functions and are small relative to the window lengths.

The approach used in (*Der et al (1993)*) is based on an implicit multichannel model of the signals received, which assumes that the signals can be described as in terms of m superposed independent processes seen on n channels. Clearly, for making the problem tractable it is required that $n > m$, i.e. that the number of channels be larger than the number of independent generalized processes. In such cases the model can be written in a partitioned form in the frequency domain for a given frequency

$$\mathbf{y} = \begin{bmatrix} y_1 \\ y_2 \end{bmatrix} = \mathbf{A} \mathbf{x} = \begin{bmatrix} \mathbf{A}_1 \\ \mathbf{A}_2 \end{bmatrix} \mathbf{x} \quad (1)$$

where \mathbf{y} is an n by 1 column complex vector of Fourier components at frequency f , \mathbf{x} is an m by 1 complex vector of the independent signal processes (assumed to have an RMS value of unity)

which vary from event to event, A is an n by m complex matrix of frequency domain transfer functions, which would also incorporate the relative amplitudes of x , that also are assumed to be nearly the same for collocated events seen at an array. Partitioning the problem such that A_1 is an m by m matrix and y_1 is on m by 1 vector, then we could, in principle, design a multichannel filter that could extrapolate y_2 from the y_1 if we knew A .

Such a filter would be obviously $A_2 A_1^{-1}$, and would exist as long as A_1 is not singular. It happens practically never because there exist some noise in the data always. We could design such a filter if we knew A , but obviously we do not know either A or x . One could also design a filter that would extrapolate the waveform on one sensor from the rest. Such a filter would work for all events with the same A regardless of the differences in x .

Nevertheless, it is possible to design such multichannel filters from the data by using the standard frequency domain formulation of the Wiener-Hopf equation

$$h = S^{-1} c \quad (2)$$

where h is the complex multichannel transfer function (an $n-1$ by 1 vector) and S is the $(n-1) \times (n-1)$ complex spectral matrix of the time series recorded at the various sensors, excluding the one to be extrapolated, and c is the $n-1$ by 1 complex column vector of the cross spectra between the $n-1$ input processes and the channel to be extrapolated. Both S and c are obviously parts of the total spectral matrix A of the array data and can be computed directly from the array recordings. As long the makeup of the signals are similar, one can compute S by averaging the cross products of the Fourier transform components over suites of n events

$$S_{ij} = \sum_n f_{in}(\omega) f_{jn}^*(\omega) \quad (3)$$

where the $*$ denotes complex conjugation. In order to weigh the various events with varying event magnitudes equally, we normalized the average absolute amplitudes of each event to the same value but kept the relative amplitudes and phases among sensors the same for the same suite of events. As long as A is nearly the same for all events, the processing using the same h will perform well for all events. In terms of physics, A can be thought of as a suite of some

transfer functions that could be interpreted as describing the site responses and relative amplitudes of generalized multipaths or multiple signals seen across the array. Coordinate rotations and intersensor propagation delays have been conveniently implicitly absorbed in \mathbf{A} and needed not be considered separately. We are not in a position to extract and interpret either \mathbf{A} or \mathbf{x} in terms of transfer functions or physical signal processes, but may still exploit the eventual similarities in the structures of quarry blast signals arriving along near identical paths. There is no guarantee that \mathbf{A} remains nearly constant for such suites of collocated events, but apparently this seems to be the case in most cases as the results below and in the original paper (Der *et al* 1993) show. The method rests on the homogeneity of transfer functions that has to be tested (Appendix A).

Typically, it is advantageous to stabilize the inversion of \mathbf{S} by regularizing it, i.e. adding to the diagonal a positive multiple of the unit matrix. Two kinds of regularizing was implemented in the code. The first consists of multiplying the diagonal elements of the spectral matrix \mathbf{A} with some factor, the second is by adding a true unit matrix which was a set multiple of the maximum of the diagonal of \mathbf{A} . We have found no visible differences in the results of the two. We have applied the first most of the time with a multiplying factor set at 1.5.

In the case where the seismic noise is a problem, in doing the waveform extrapolation, the Wiener filters can be modified by including the noise spectral matrix \mathbf{N} in the design

$$\mathbf{h} = (\mathbf{S} + \mathbf{N})^{-1} \mathbf{c}. \quad (4)$$

In order to do this one needs to estimate \mathbf{N} from the seismogram preceding *each individual* event to be processed. This way the process can be optimized for the given background noise field. Obviously it is advantageous from the reliability point of view to estimate \mathbf{S} and \mathbf{c} separately from high S/N events and design \mathbf{h} from the formula prior to applying it to any low S/N events.

Time Domain Approach

The scheme of identifying a regional arrival type from the comparison of an extrapolated sensor output to an actual one can be reduced to a statistical testing of a set of residuals to

determine which one of the regional phase models, defined in terms of multichannel filters, is the most likely one. This is similar to the schemes described by *Basseville and Nikiforov (1993)* to determine which of a set ARMA models fits a set of data best. The residuals of extrapolation of one output from the rest can be written as

$$\varepsilon_{k,i} = s_{k,i} - \sum_{j \neq k} \sum_{l=-N}^{l=N} s_{j,i-l} f_{j,l} \quad (5)$$

where $f_{i,j}$ are the filter weights applied to the traces $s_{i,j}$ with the first sum over all sensors excluding the sensor output k to be extrapolated from the rest. The length of the time-symmetric filter is $2N+1$. The weights can be obtained by solving the well-known time domain multichannel filter design equations (*Wiggins and Robinson 1965*), where the r_i are

$$\begin{bmatrix} r_0 & r_1^T & r_2^T & . & . & . & . \\ r_1 & r_0 & r_1^T & r_2^T & . & . & . \\ r_2 & r_1 & r_0 & r_1^T & r_2^T & . & . \\ . & r_2 & r_1 & r_0 & . & . & . \\ . & . & r_2 & . & . & . & . \\ . & . & . & . & . & . & . \\ . & . & . & . & . & . & r_0 \end{bmatrix} \begin{bmatrix} f_1 \\ f_2 \\ f_3 \\ . \\ . \\ . \\ . \end{bmatrix} = \begin{bmatrix} g_1 \\ g_2 \\ g_3 \\ . \\ . \\ . \\ . \end{bmatrix} \quad (6)$$

block $k \times k$ autocorrelation matrices, subscripts are for each time lag i , where k is the number of input traces, and the g_i are the cross correlation vectors between the inputs and the trace designated as the desired output, and f_i are filter weights. The large matrix is block-Toeplitz in form and is thus amenable to iterative solution methods. These can be obtained by ensemble-averaging the corresponding correlation functions over suites of collocated events for each specific arrival. The weights will be specific to each arrival the sample windows will be centered on. We have implemented the recursive algorithm of *Wiggins and Robinson (1965)* for use in our work.

The correlation functions were computed in a manner similar to the spectral matrices above by summing the cross-correlation functions among sensor pairs of the various events after RMS event-normalization of the waveforms to avoid the domination of the cross-correlation function matrices by the events with the largest magnitudes.

DATA ANALYSIS

Frequency Domain.

The time domain method as described above was applied to various data sets. The “mini-array” consists of a three-component set at A0 site of ARCESS combined with three vertical sensors in the C ring (**Figure 10**). Applying the multichannel waveform equalization method to the two sets of data results in good replicas of the waveforms of all phases. **Figures 11 to 14** show the results for some examples of Pn, Pg, Sn and Lg for the original K2 data set.

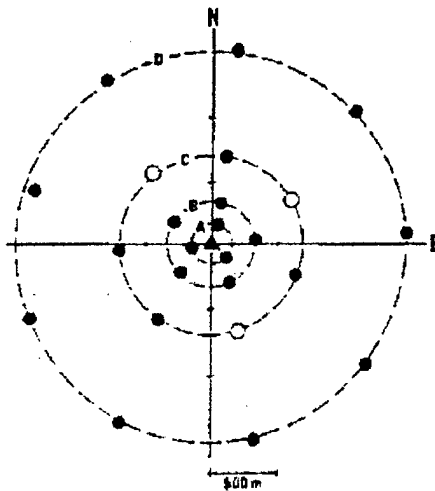


Figure 10. ARCESS array configuration.

```

d:k2054.dat
ccf 9.472633E-01
End...

```



```

d:k2110.dat
ccf 9.770098E-01
End...

```



```

d:k2102.dat
ccf 9.228188E-01
End...

```



Figure 11. Examples of Pn waveform extrapolations using the “mini-array” and the leave-one-out method. All of the waveform matches between the original A0 waveforms (top) and the waveform extrapolations (below) are excellent. Event identifications and correlation coefficients are plotted above each pair of waveforms. The waveform sections shown are 6.4 seconds long.

```
d:k209.dat  
ccf= 0.698682E-01  
End...
```



```
d:k210.dat  
ccf= 9.826458E-01  
End...
```



```
d:k2132.dat  
ccf= 7.877706E-01  
End...
```

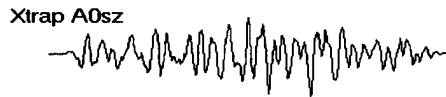


Figure 12. Pg waveform extrapolations using the “mini-array” and the leave-one-out method. All of the waveform matches between the original A0 waveforms (top) and the waveform extrapolations (below) are good. Event identifications and correlation coefficients are plotted above each pair of waveforms. The waveform sections shown are 6.4 seconds long.

```

d:k2054.dat
ccf= 7.495535E-01
End...

```



```

d:k2118.dat
ccf= 7.158732E-01
End...

```



```

d:k2132.dat
ccf= 6.911626E-01
End...

```

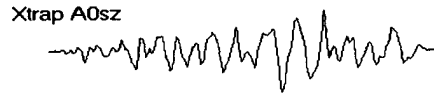
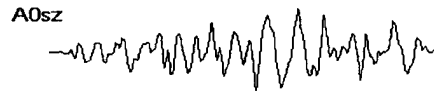


Figure 13. Sn waveform extrapolations using the “mini-array” and the leave-one-out method. The waveform matches between the original A0 waveforms (top) and the waveform extrapolations (below) are reasonably good. Event identifications and correlation coefficients are plotted above each pair of waveforms. The waveform sections shown are 6.4 seconds long.

```

A0K2054.dat
ccf 0.458871E 01
End

```



```

A0K2118.dat
ccf 0.379412E 01
End

```



```

A0K2182.dat
ccf 6.761250E 01
End

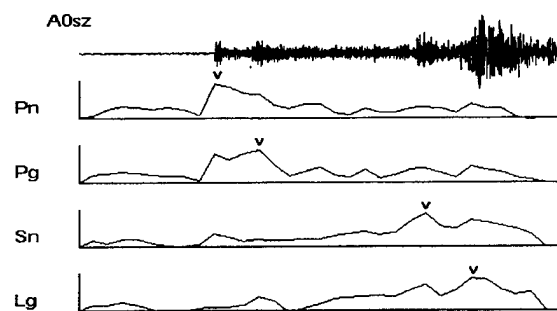
```



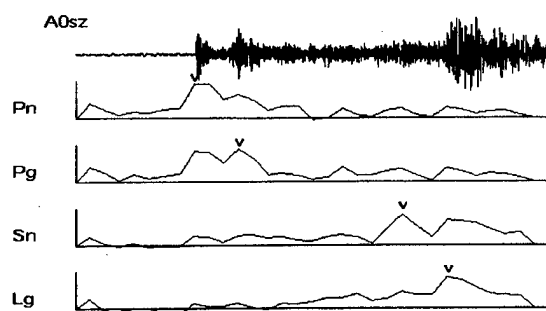
Figure 14. Lg waveform extrapolations using the “mini-array” and the leave-one-out method. For this arrival The waveform matches between the original A0 waveforms (top) and the waveform extrapolations (below) are still good but for a few events the correlation coefficients are low, such as the one pair at the bottom. Event identifications and correlation coefficients are plotted above each pair of waveforms. The waveform sections shown are 6.4 seconds long.

The complete runs on events were performed the following way. The frequency domain filters were computed from the event-compounded spectral matrices of a learning data set. These filters were applied, in the frequency domain, over half-overlapping 256 point windows over the whole recording to construct the extrapolated reference trace arbitrarily chosen to be the vertical at site A0. Normalized correlation coefficients were then plotted as a function of time for the four filter outputs designed to extrapolate the wavefields appropriate to Pn, Pg, Sn and Lg. Note that the information makes no use at all of the variations in the absolute amplitudes of the input which define a regional arrival to an analyst. Neither does the increase of correlations at the arrival of Pn has anything to do with the increase of wave amplitudes at that time. This increase of correlation coefficients would occur even if the amplitudes did not change. It merely shows that the motion is more "Pn-like" in the windows than in the windows preceding it.

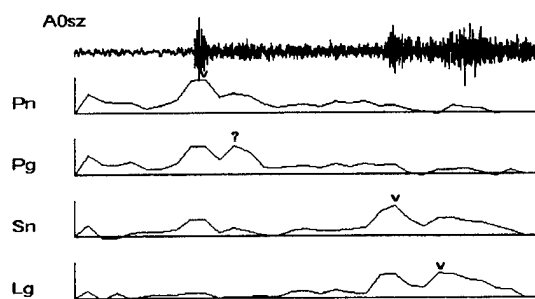
Inspecting the results of complete processing runs on some complete events show that, in general, it is possible to distinguish between Pn and Pg, and Sn and Lg in most cases. There is no ambiguity in telling the P type and S type phases apart. While Pn is the first maximum on the Pn runs, Pg may be still smaller than Pn in the Pg runs, but it is generally more pronounced and enhanced relative to Pn in the Pg run. **Figure 15** shows results for some events in the K2 mine.



Event K2054

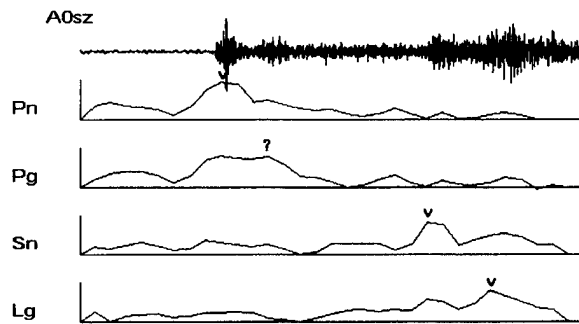


Event K2110



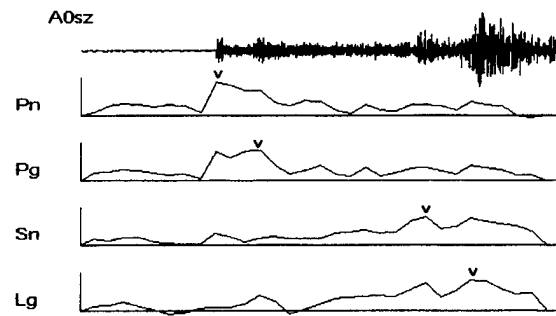
Event K2219

Figure 15.

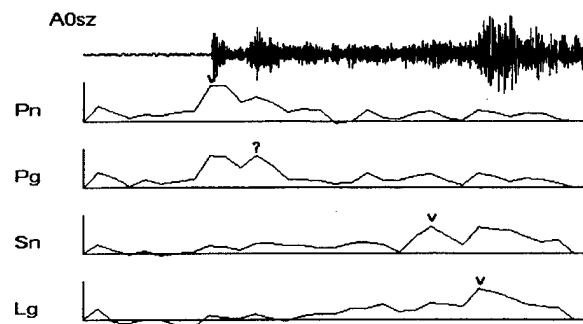


Event K2285

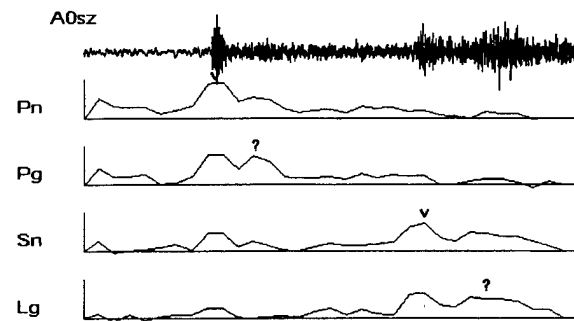
Figure 15. Processed events from the K2 mine using the "mini-array" configuration. The seismogram of the A0 sensor is shown on top. The correlation coefficient between 256 point (6.4 sec) half-overlapping windows on the A0 trace and the extrapolated waveform is plotted as a function of time along the time axis. The vertical line segments on the left indicate the 0-1.0 range in the size of correlation coefficients. The results for filter sets designed to identify Pn, Pg, Sn and Lg are plotted from top to bottom. Note that the maxima tend to occur at the right arrivals (v marks). Often the Pg (or other phase) is identified only by a large increase, not an absolute maximum, at the time of the arrivals o (? Marks). Nevertheless, such increases often identify the phase well. The total length of the records processed in this type of figure was 102.4 seconds throughout this report.



Event K2054

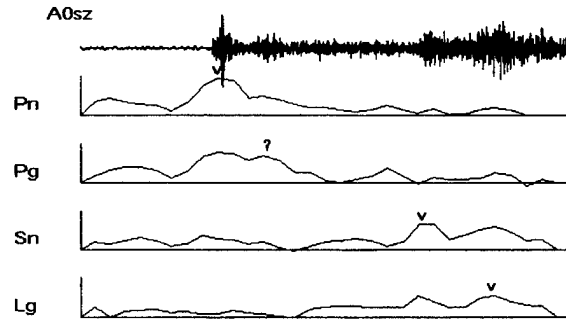


Event K2110



Event K2219

Figure 16.



Event K2285

Figure 16. K2 events processed by the leave-one-out technique. In these runs we have excluded frequencies below 1 Hz, where the background noise dominates and/or it is similar to the Pn because of the longer wavelengths. This exclusion from the processing was effected by not using these low frequencies in the waveform reconstruction. The resulting small loss in the size of correlation coefficient apparently was not serious. Length of these time traces is 102.4 seconds.

An important question, since we are doing no spectral smoothing is, how many events are needed for the scheme to work. In order to test the robustness of the scheme, we have made runs with the K2 data set where the event being processed was excluded from the training data set used for computing the filters. These processing runs still identified the appropriate arrivals quite well (**Figure 16**) with some exceptions for Lg. In general, Pn waveform extrapolations were quite robust when the leave-one-out method was applied, but the robustness decreased from Pn to Lg. It appears that one should not use much less than nine events as a learning set. These should be in the same general area, but need not be in the same quarry (*Der et al 1993*).

It is interesting to inspect the time domain equivalents, impulse responses, of the filters being used for identifying Pn, Pg, Sn and Lg. In **Figures 17-20** we show these for the K2 mine. These show that in a sense what we are doing is similar to beamforming. The highest amplitude portions of the impulse responses follow approximately the propagation time delays appropriate to the phases. Note that these delays increase from Pn to Lg. Nevertheless, in pure beamforming we should have only delayed delta functions with zeroes in between, while our responses are quite complex, and thus we are doing a complex filter-sum instead of delay sum. It is interesting to note that for Pn reconstruction, we now use mostly the available C ring vertical sensors, largely ignoring the horizontal components, while in Paper I we have shown that the two horizontal components of motion at A0 can accomplish the same goal quite well.

When regularizing the spectral matrices we have constrained the processor such that it does the least amount of waveform transformation to accomplish the goal of effective wavefield extrapolation.

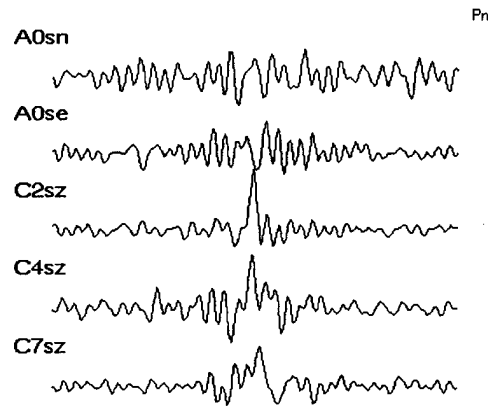


Figure 17. Impulse responses of filters designed to extrapolate the Pn wavefield for events at the K2 mine using the “mini-array” from ARCESS. The zero-lag time is at the middle of each waveform. Time length of these impulse responses is 6.4 seconds.

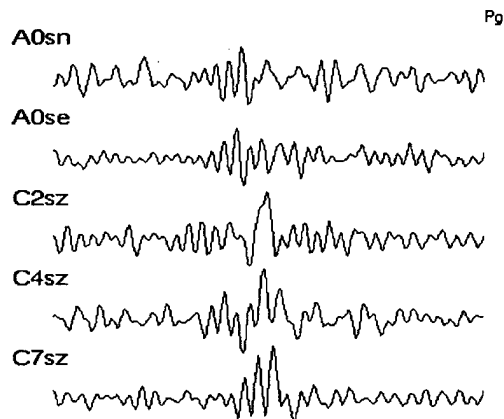


Figure 18. Impulse responses of filters designed to extrapolate the Pg wavefield for events at the K2 mine using the “mini-array” from ARCESS. Time length of these impulse responses is 6.4 seconds.

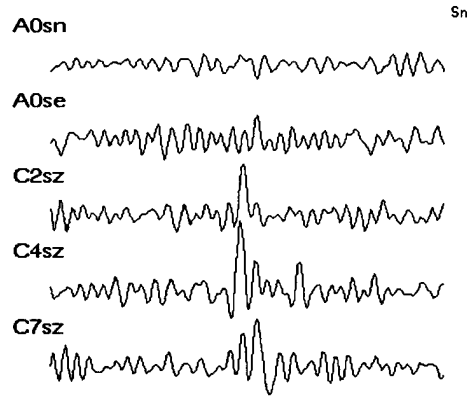


Figure 19. Impulse responses of filters designed to extrapolate the Sn wavefield for events at the K2 mine using the “mini-array” from ARCESS. Time length of these impulse responses is 6.4 seconds.

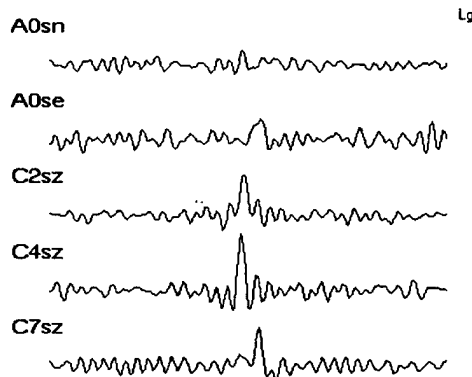
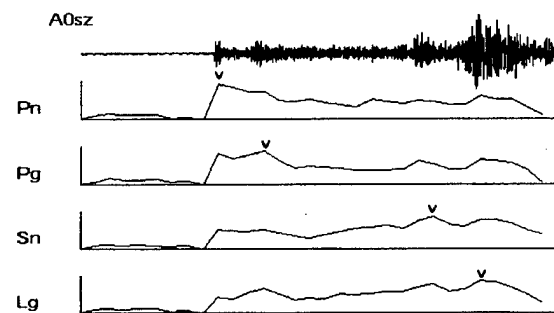


Figure 20. Impulse responses of filters designed to extrapolate the Lg wavefield for events at the K2 mine using the “mini-array” from ARCESS. Time length of these impulse responses is 6.4 seconds.

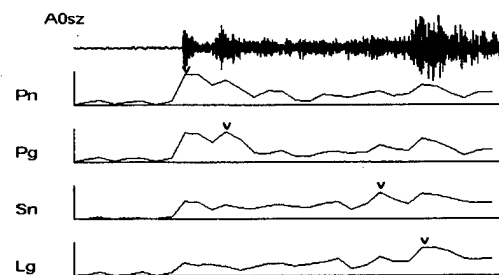
As an alternative sensor configuration we have also evaluated a combination of three sensors of the C ring, the vertical sensor at A0 and two vertical sensors in the B ring. (many of these choices were dictated by the availability of data channels without errors). We have recovered data for this combination for all the Kola mines except K3. This configuration has the drawback of small effective aperture, but it discards the two horizontal components at the center that are not effectively utilized (as revealed by **Figures 17-20**) for the later arrivals in the “mini-array”, especially Sn and Lg. In retrospect, a better configuration could consist of the vertical sensors

of the whole C ring combined with the vertical sensor at A0.

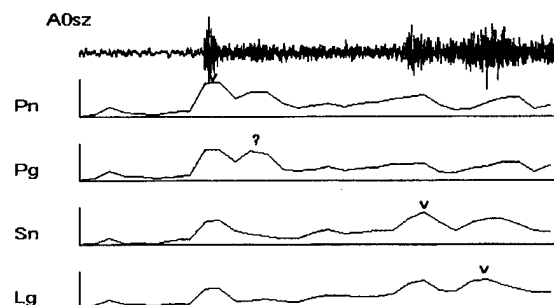
The runs for this configuration again show the effective identification of the four major arrivals (**Figure 21**) for the K2 mine, but the differences among them are less pronounced. The beamforming has less discrimination power, because of the closeness of A0 to the B ring sensors. Nevertheless, in such processing although we are giving more weight to the closest sensors in extrapolating a sensor output from the rest, this is not simple copying-over with a time delay. Actually, it can be verified by inspection of the extrapolated traces that they are better reproductions of the A0 waveform than the waveforms seen at the nearest B ring sensors.



Event K2054

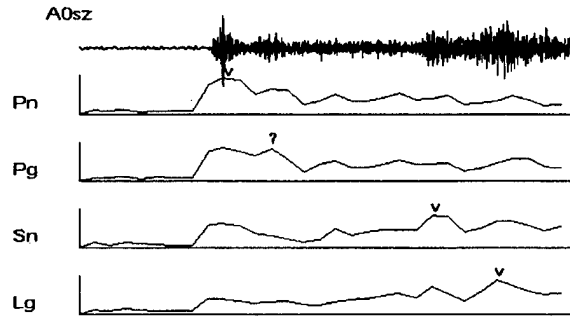


Event K2054



Event K2219

Figure 21.



Event K2285

Figure 21. Processed events from the K2 mine using the all-verticals configuration.

The impulse response of the filters show that the B ring sensors, which have waveforms closest to that of A0, are used with the greatest weights (**Figures 22 to 25**). The relative weighting and the filter waveforms are quite complex

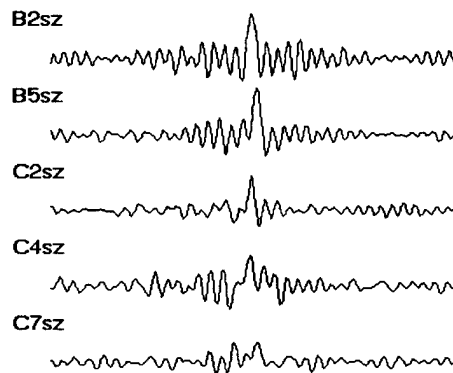


Figure 22. Impulse responses of filters designed to extrapolate the Pn wavefield for events at the K2 mine using the all-vertical array from ARCESS. The zero-lag time is in the middle of each waveform. Time length of these impulse responses is 6.4 seconds.

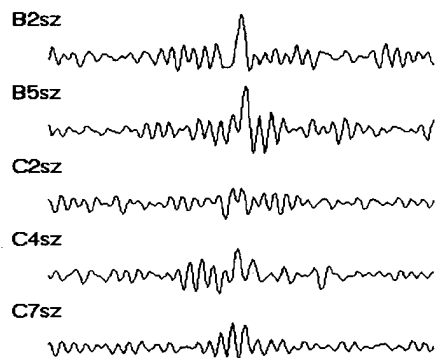


Figure 23. Impulse responses of filters designed to extrapolate the Pg wavefield for events at the K2 mine using the all-vertical array from ARCESS. The zero-lag time is in the middle of each waveform. Time length of these impulse responses is 6.4 seconds.

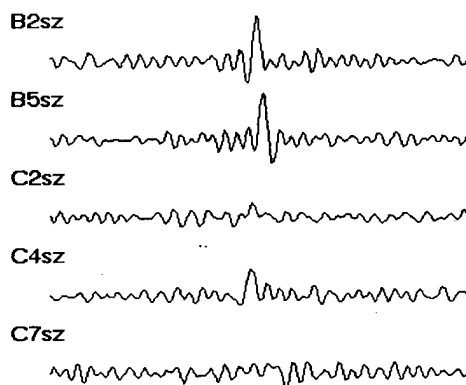


Figure 24. Impulse responses of filters designed to extrapolate the Sn wavefield for events at the K2 mine using the all-vertical array from ARCESS. The zero-lag time is in the middle of each waveform. Time length of these impulse responses is 6.4 seconds.

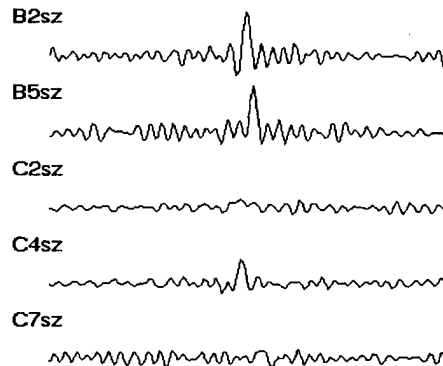
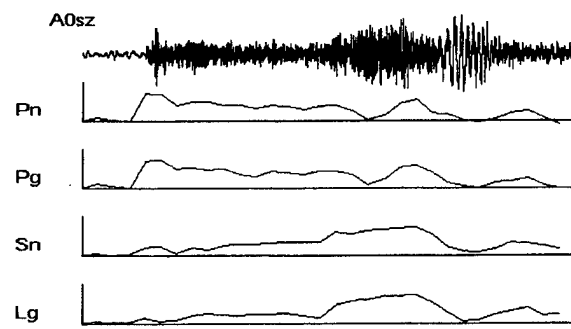
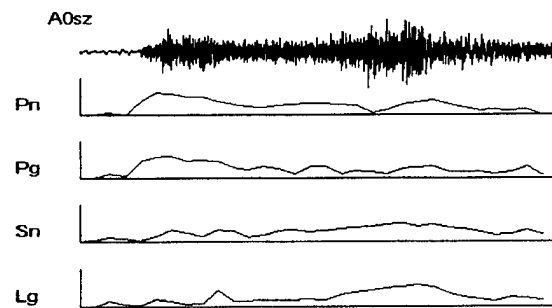


Figure 25. Impulse responses of filters designed to extrapolate the Lg wavefield for events at the K2 mine using the all-vertical array from ARCESS. The zero-lag time is in the middle of each waveform. Time length of these impulse responses is 6.4 seconds.

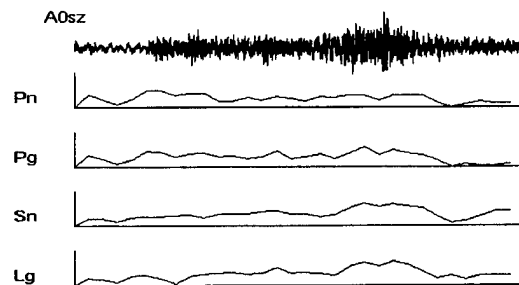
We have done some tests in using the filters designed for one mine (using the all-vertical array in all these tests) on events of the other mines. Remembering the reported locations of the events the K1, K2 and K5 mines appear to be located closer than the K4 and K8 mines (if these locations can be believed). When the filter set of K2 is applied to the events of K4 mine the correlations are lower and it is no longer possible to see any differences in the Pn and Lg pair or the Sn and Lg pair (**Figure 26**). Nevertheless, P and S type phases still produce maxima in different parts of the seismogram. This was expected based on the different azimuth and distance of the K4 mine.



Event K4118



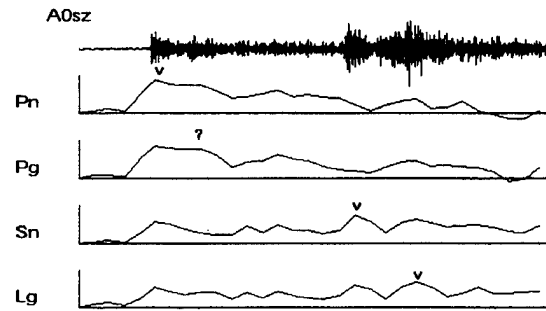
Event K4244



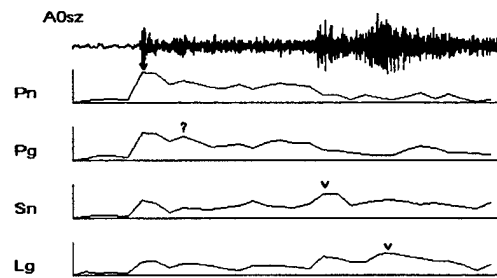
Event K4270

Figure 26. Results of filtering K4 events with a filter designed for K2 mine. The phase identifications are poor or non-existent. Length of these traces is 102.4 seconds.

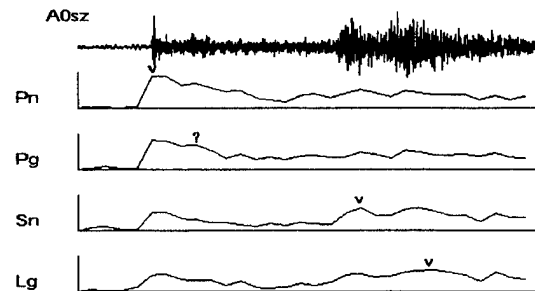
On the other hand, applying the filters designed for the K2 mine to events in the K1 and K5 mines the phase identification was not entirely unsuccessful (**Figures 27 and 28**), which was also expected based on their similar locations.



Event K1189

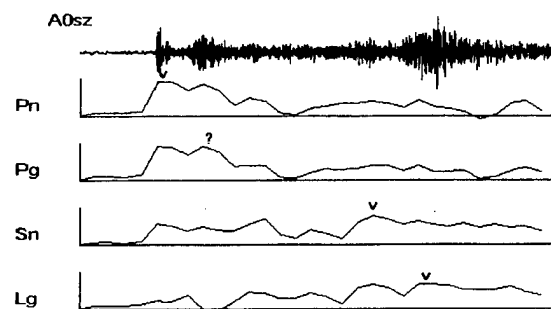


Event K1280

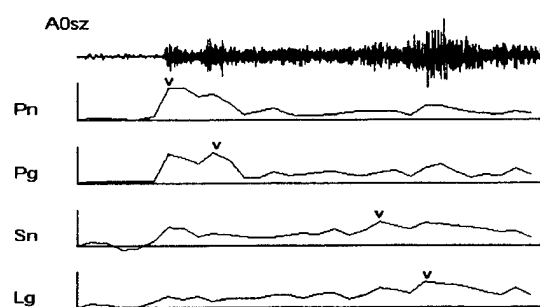


Event K1301

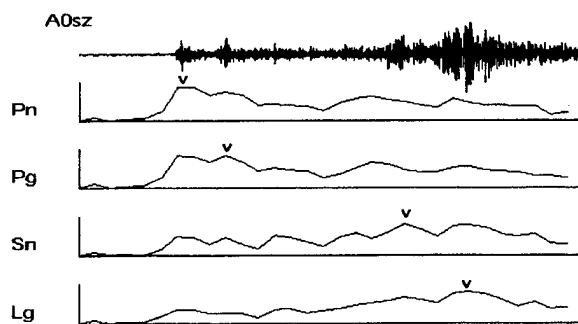
Figure 27. K1 mine events processed with the filter set designed from K2 mine data.



Event K5040

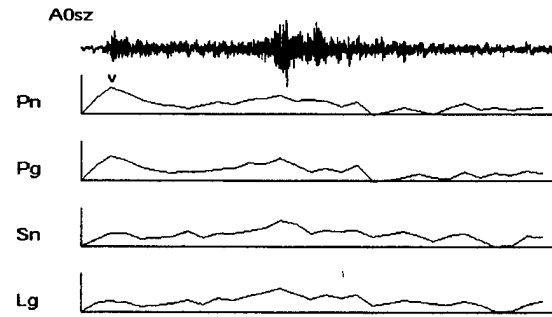


Event K5222

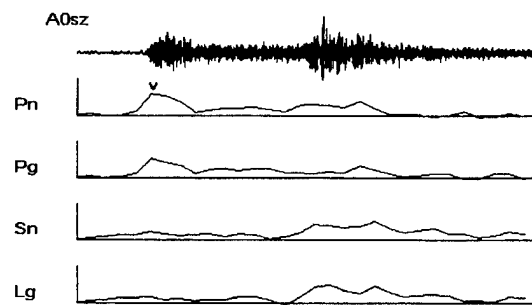


Event K5278

Figure 28. K5 mine events filtered with a set of filters designed for K2.



Event K8178



Event K8223

Figure 29. K2 filters applied to K8 mine events.

On the other hand, application of the K2 filters to the events at K8 is again a total failure (**Figure 29**). We still are able to tell the P and S type phases apart, but there is no Pg or Sn, and they are also unclear in the original seismograms.

Time Domain

Much of the work was spent on developing a frequency-domain implementation of the regional phase identification method of *Der et al (1993)*. Thus, we transformed the frequency domain filters that equalize the waveforms into the time domain. These will be applied as convolution filters in a continuous fashion. A drawback of this approach is that these filters are non-causal and introduce precursors. Nevertheless, since our purpose is phase identification and the precursors have very little energy, this is not a problem.

As described by *Der et al (1993)*, we design digital filters for predicting, or more correctly, extrapolating the center vertical seismometer waveform from the rest of the mini-array (two collocated horizontals and a tripartite configuration of vertical from the C ring) based on the event compounded spectral matrix derived from a set of events. The filters then can be applied to individual, collocated events, even those not including the learning set. The success of the waveform extrapolation identifies the phase on which the filter was designed. We have concentrated on the Pn and Lg phases which we regard as the key phases in locating an event. The same approach can, and has been, applied to other identifiable regional arrivals as well, such as Sn and Pg (*Der et al 1993*).

We show the time domain filters for the extrapolation of Pn phase waveforms in **Figure 30A**. These were designed by inverse Fourier transforming the frequency domain filters in *Der et al (1993)* and tapering off the ends. These filters are quite complicated, but the relative amplitudes show that it is mostly the two horizontal components that contribute to the prediction. The forms of filters do not lend themselves to easy intuitive interpretation since the observed waveforms, being influenced by distortion due to local geology, are quite complex themselves. Nevertheless, the details of original and predicted Pn waveforms (**Figure 30B**) are quite similar, and their cross-products, which would contribute to the cross-correlation coefficients, are predominantly positive in polarity (lowermost traces). **Figure 30C** shows the original A0 vertical compared to the prediction and the smoothed cross-product for the whole recording of the same events. In this display no normalization with respect to the power in the traces of the cross product has been performed and the relative amplitudes of various arrivals still play a role. Nevertheless, it is clear that the processing enhances Pn relative to the other phases, even in the cases (not shown) where Lg was much stronger than Pn.

Similarly, the filters designed to process the Lg phases are also much more complex than one would expect for simple beamforming, since such filters would contain only a few spikes at the correct time lags. In this case the main contributions come from the rest of vertical traces (**Figure 31A**). The original and predicted Lg waveforms are quite similar again in many details (**Figure 31B**) and their cross-products are again predominantly positive. The waveform matching procedure did not work as well for Lg as for Pn. **Figures 31C** show the original A0 vertical compared to the prediction of Lg and the smoothed cross-product for the whole A0 sensor recordings of the same events. It is clear that the processing enhanced Lg considerably relative to the other phases. Not all of the processed events show enhancement of Lg only as shown here, however, some enhance Sn as well. This can be expected, since both Sn and Lg contain considerable SV components.

The performance of filters designed entirely in the time domain using correlation functions and the recursive block Toeplitz matrix inversion procedure (*Wiggins and Robinson 1965*) was comparable to the results presented above for Pn even when very short 31 point filters were used. The advantage of such approach is that the filters thus designed are optimum for their time length, instead of being truncated as above. The finding of the most effective and parsimonious filter lengths is the subject of our ongoing work. For Lg the short filters did not work well, we are presently modifying and testing the program to compute longer time domain filters, but shorter than the 160 point filters shown above. The need for testing this is dictated by the fact that the computation of longer filters may make the recursive algorithm become unstable.

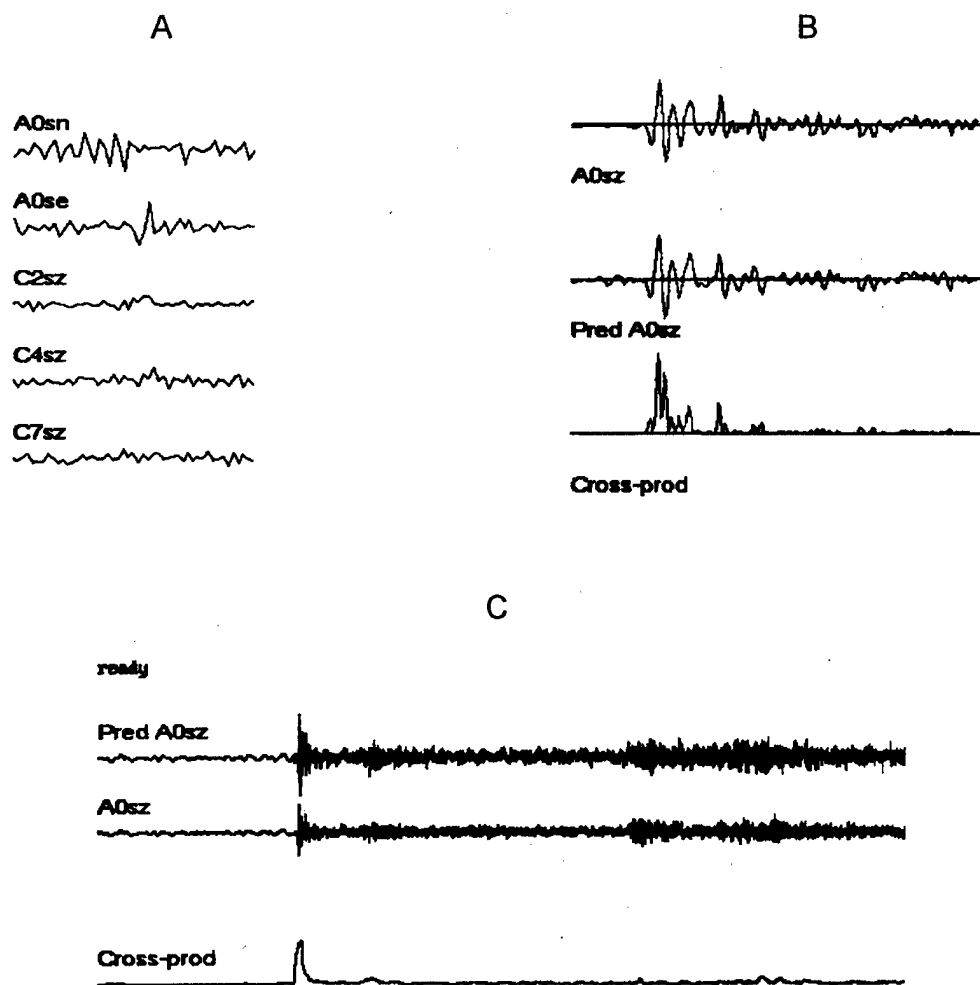


Figure 30. A) Time domain filters for the enhancement of Pn, length 160 points=4 seconds. B) Detail of A0 Pn waveform for event 1990219 (top) vs. the predicted one (middle) and their cross product (bottom). Time length 6.4 seconds. C) Processed trace (top), actual seismogram (middle) and the leaky-integrated cross product. Time length 102.4 seconds.

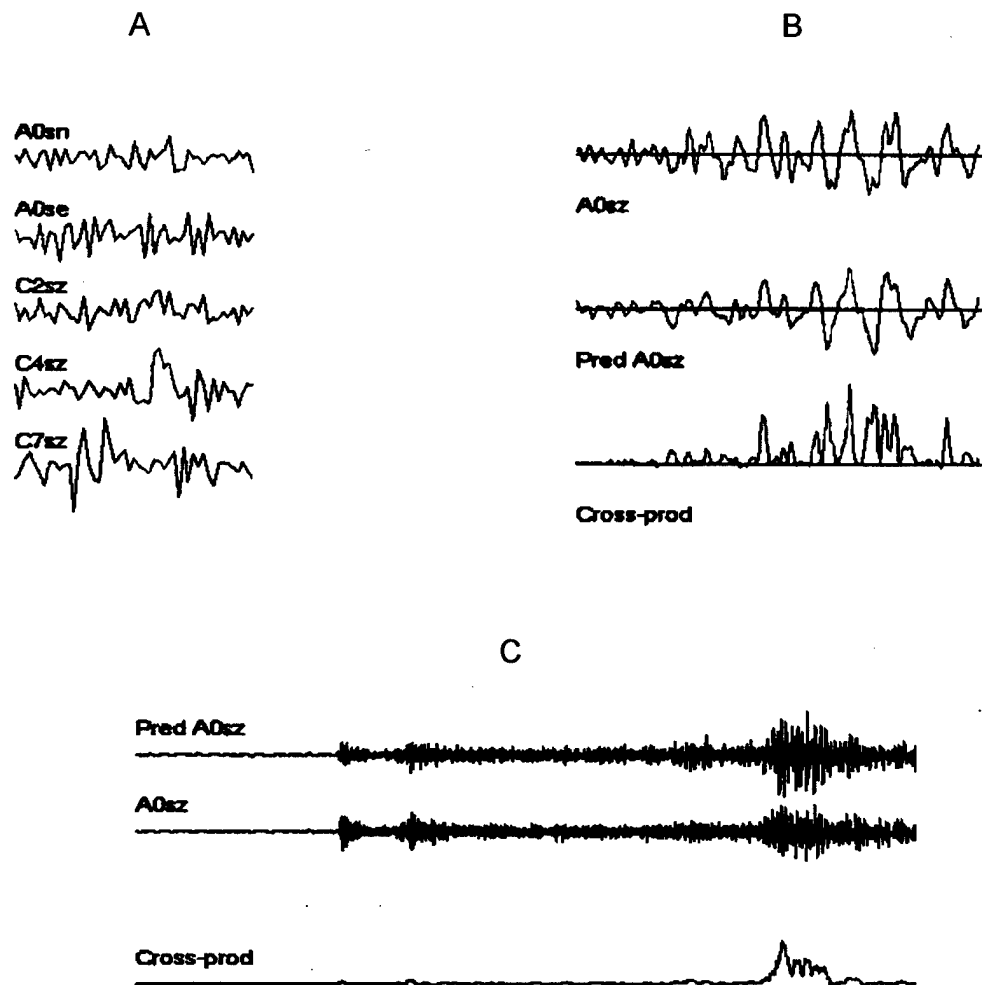


Figure 31. A) Time domain filters for the enhancement of Lg, length 160 points=4 seconds. B) Detail of A0 Lg waveform for event 1990110 (top) vs. the predicted one (middle) and their cross product (bottom). Time length 6.4 seconds. C) Processed trace (top), actual seismogram (middle) and the leaky-integrated cross product. Time length 102.4 seconds.

SUMMARY OF POLARIZATION PROCESSING RESULTS

The generalized polarization method for automatically identifying regional arrivals appears to be successful for groups of events that are close in their back azimuths and slownesses of their phases at a small array, but not necessarily closely spaced in the absolute sense. Such event groups may be actually scattered over distances of several tens of kilometers when the array to event distances are of the order of 350 km. Gross features of the generalized polarization filter operators can be explained in terms of the conventional concepts such as slownesses and body wave polarizations, but in more detail they are quite different. The technique breaks down as the events scatter over larger areas. The method seems to remain stable when the event to be processed is left out from the suite used to design the processor. The efficacy of the process seems to degrade, however, from Pn to Lg. This is probably caused by the greater complexity, in terms of modes or signal processes, of the later arrivals.

PHASE ARRIVAL TIME ESTIMATION AT REGIONAL DISTANCES USING THE CUSUM ALGORITHM

Introduction

Automatic phase arrival time estimation is of considerable interest because of the need for rapid location and identification of numerous seismic events by networks monitoring natural and man-made seismic activity. Times of seismic "phase" arrivals are defined as times where some visible characteristic, such as amplitude, frequency content or wave polarization changed in some recording. Typically, regional arrivals are high frequency, broadband, emergent wave groups containing numerous cycles. Later arrivals generally have no clear, impulsive waveforms and are preceded by the codas of earlier ones, and their onset times can only be defined to within a few cycles.

A human operator often can spot arrivals by noticing subtle changes in the frequency content in noisy records. On the other hand, when such human capabilities are needed, it simply indicates a failure of applying appropriate frequency domain prefiltering that could have already produced an enhanced amplitude contrast between the noise and the arrival. Once the amplitude contrast is enhanced, the contrast in frequency content will be much less noticeable. Appropriate prefiltering in frequency is a prerequisite for further onset time determination regardless whether it is manual or automatic. Various schemes for optimum pre-filtering were suggested and most of these seem to work well. Kvaerna's definition of "usable bandwidth" (Kvaerna 1995, 1996a) and S/N^2 (in amplitude) or noise-adaptive predictive filtering enhances the amplitude contrast between the noise background preceding the onset of the signal at the expense of decreasing the visible frequency contrast between the signal and noise. Thus, according to experience in noisy signals thus processed it is hard to spot the signal arrivals by the changing frequency content. The biggest visual differences between the signal and noise parts of raw regional seismograms are due to the presence of low frequency microseisms, which are eliminated by the prefiltering processes. To illustrate this point, in **Figure 32** we show examples of S/N^2 filtered signals and noise and in **Figure 33** simple 2.5-14 Hz band-pass filtered signals which both emphasize the usable bandwidth. None of these examples show any noticeable changes in the frequency content upon the arrival of the signals, and the signal arrivals are noticed only because of the changes in the average trace amplitudes.

Automated equivalents of subjective human operations requires the definition of some statistics (e.g. amplitude, AR model, polarization parameters) and some algorithm that can define the time when such parameters changed. The standard short-term average over long-term average ratio (STA/LTA) algorithm is well suited for arrival detection but not for precise arrival time estimation because of the long delay associated with any significant change in the STA. Most methods proposed for precise arrival time estimation typically attempt to detect the first point where some statistic suddenly changes. Many of these may work for most first arriving Pn if the signal is impulsive, but do poorly with emergent phases or secondary arrivals typically seen at regional distances. The situation is more difficult in picking the later arrivals in regional seismograms. In that case there is little or no frequency contrast. Typically, the spectra of the various regional arrivals are quite similar, for quarry blast sources they are nearly *identical* (Baumgardt and Ziegler 1986). There are, thus, no spectral differences to exploit and the determination on onset times must depend mostly on amplitude or polarization changes."

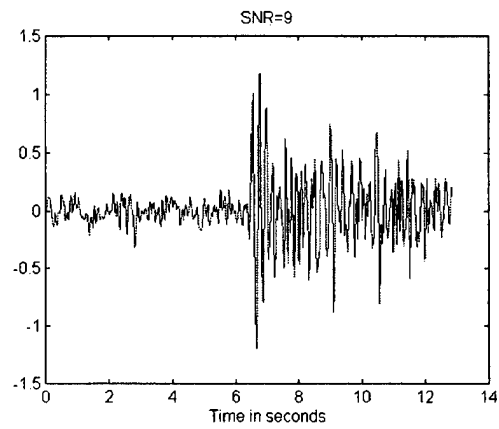
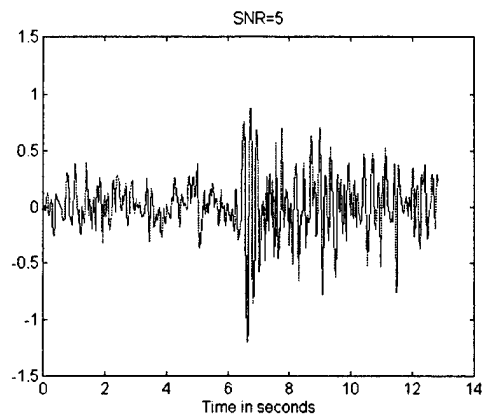
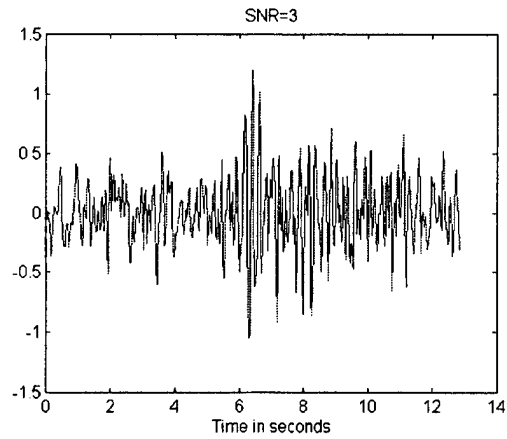


Figure 33. S/N2 filtered signals with various S/N ratios.

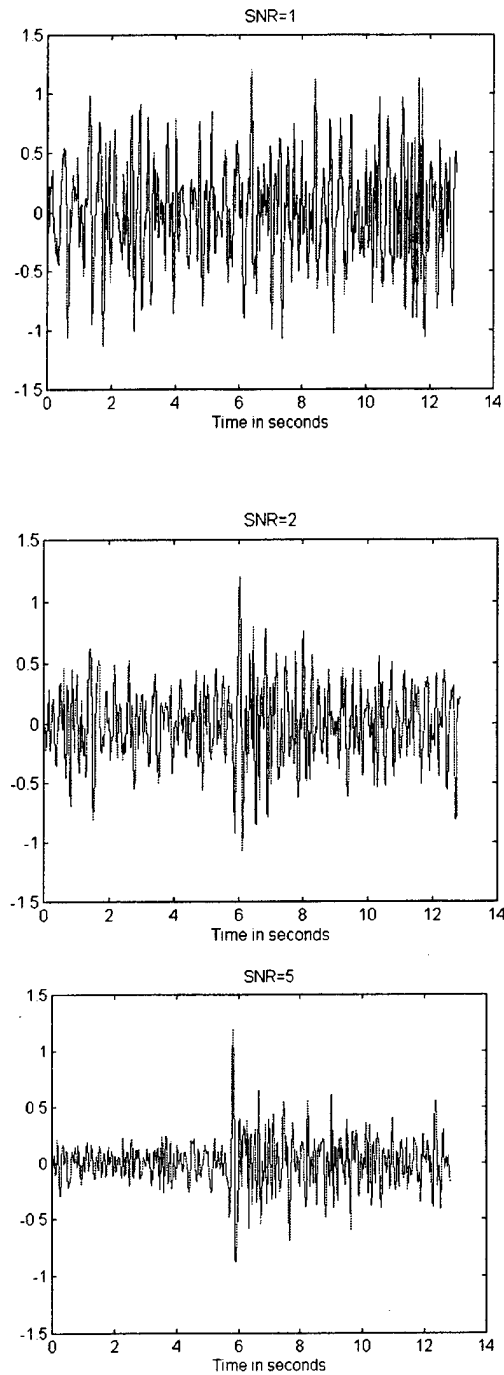


Figure 34. 2.4-14 Hz band-pass filtered signals with various S/N ratios.

There is a basic philosophical issue associated with the definition of regional "arrival" onset times. Typically, most current routine analyst-guided processing is based on the picture of regional seismograms being made up of a few phases such as Pn, Pg, Sn and Lg typical of Scandinavia and Europe. Analysts are trained to recognize and pick these particular arrivals. Numerous studies have shown, however, that regional seismograms are much more complex and could, more appropriately, be described in terms of various physically meaningful wave groups such as various guided wave groups and reflections such as multiple PmP and SmS (*Vogfford and Langston 1990*). An automatic processor will thus find more arrivals than an analyst indoctrinated in the Pn-Pg-Sn-Lg framework and these may not exactly correspond. This will be even more true for seismograms recorded in tectonic-geologic environments different from Scandinavia which may be quite different. In cases of such conflicts the automatic processor may often be right and the analyst wrong. In this report, we still use the Pn-Pg-Sn-Lg framework only because it seems to fit the data, not because we have a faith in the absolute global validity of it.

Accurate onset time determination is important because the accuracy of regional location depends on errors in the onset time picks. If the onset of Pn is well above the background noise level (after appropriate frequency filtering), the associated onset times should be used in location. On the other hand, Pn often has lower amplitudes than some of the later arrivals. In such cases later arrivals must be utilized. Moreover, the ability to determine onset times of later arrivals automatically is useful for the following reasons: first, it helps to identify the nature and approximate distance of the event by the pattern of envelope amplitudes and onset times, second, some of the regional spectral discriminants based on spectral ratios of various wave groups can be applied automatically.

A related issue of practical importance is that of the late onset time picks for emergent signals buried in high background noise. Many body wave arrivals start with a small precursor or build up in amplitude gradually. In such cases the beginning of the signal is missed and the onset time estimate will be late (*Kvaerna 1996a,b, Douglas et al 1997*). In our opinion this situation has no remedy, because, as we shall show below, both the analyst and any automatic processor will pick the onset time late.

The CUSUM algorithms described in *Basseville and Nikiforov (1993)* were designed for pinpointing the time of a change in a system and have their primary applications in quality control and machine diagnostics. The basic idea is detecting changes in the trends of the cumulative sum of some suitable statistic that abruptly changes with time as the properties of the time series change. It is much easier to see and quantify a change *in a trend*, than to pinpoint the exact time of the *first point* where the change occurred. The most appropriate statistic to be used depends on the particular change to be detected and will be varied. In the case of seismic arrival onset determination case we look for changes in signal amplitudes, spectral contents (AR model residuals) and polarization (cross-extrapolation residuals) or any combinations of these. The CUSUM-based methods have indeed been used for determining P onset times in the past (*Nikiforov and Tikhonov 1986, Nikiforov et al 1989*), but not in a combination with simulated annealing as below.

A simple application of the method is to compute the cumulative sum of the chosen statistic and subtract a linear ramp from it. This way the changes in the trend of the CUSUM are converted to minima. Numerous methods for automatic finding of minima for empirical functions exist. The simplest is to find absolute minima in the time windows where the arrival times of phases were expected. Such time windows can be provided by the generalized polarization analysis method described in the first part of this report. This method, although crude, seems to be quite successful (**Figures 35 and 36**). These are results for the Khibiny data set (*Mykkeltveit, S. 1992*).

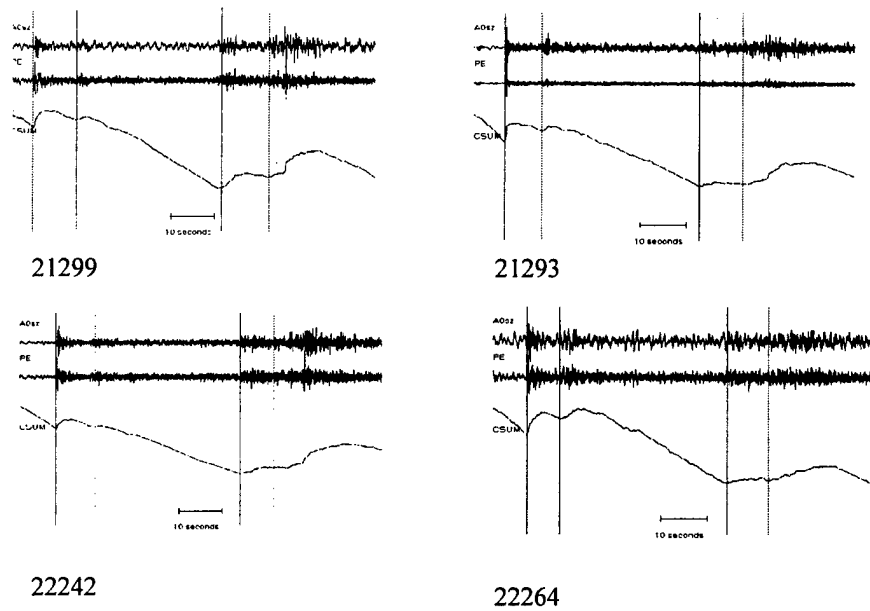


Figure 35. Application of the CUSUM method to four events in the Khibiny data set. The top trace is the original single sensor output, below it is the adaptive AR filtered version. At the bottom is the cumulative sum of the absolute values of the second trace with the time picks (vertical lines) for Pn, Pg, Sn and Lg. Note that in spite of the ill-defined beginnings of each phase the minima are quite well defined. Absolute minima in certain time frames were picked. These examples of onset time estimation are based on amplitude changes of course.

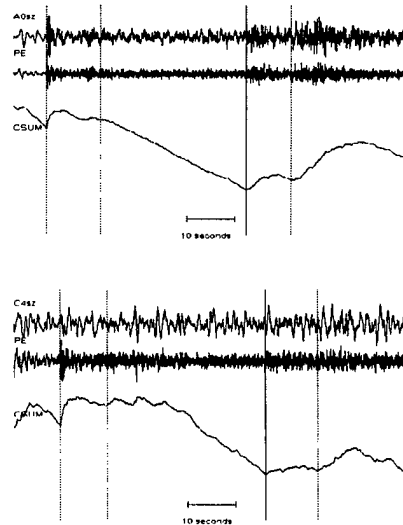


Figure 36. Application of the method to two more events picking absolute minima of CUSUM.

Combining CUSUM with Simulated Annealing.

Instead of finding an absolute minimum in the CUSUM-linear trend sum, the minimum could also be located by some randomized search method. Simulated annealing is such an optimization technique which is designed to find global minima of irregular functions where many local minima may exist. It tends to disregard minor local minima and converge to the lowest points. It uses the random Metropolis search algorithm which is based on a thermodynamic analogy (*Press et al 1986*). Initially, it allows the search using large steps in the independent variables which may even be associated with increased values of the function. This allows the solution to “jump out” from local minima and resume search for other minima. As “cooling” occurs such steps are accepted less and less and finally the solution will settle in broad global minima.

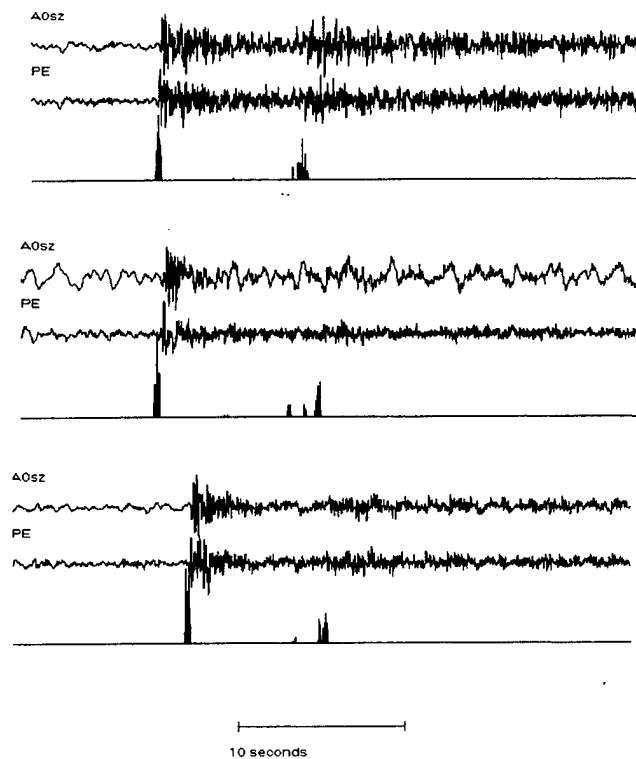


Figure 37. Very tight arrival time pick clusters were obtained using repeated applications of simulated annealing. These are processing results on ARCESS data for Kola events. Time length 102.4 seconds.

Since there is a possibility that occasionally local minima may be located, a few rules are needed to restart the algorithm. The algorithm is extremely fast and can be run many times to narrow down on the actual arrival times and assess their mean error empirically (**Figure 37**).

The examples in **Figure 37** are displays of histograms of 300 independent SA searches vs. the original and AR filtered seismograms. We are attempting to pick the emergent Pn and Pg phases on SPZ seismograms from the CUSUM. Note that most clusters of the picks correspond to where a seismologist would see arrivals. The variability in individual clusters of solutions can be used to assess the average scatter in travel time picks. These are processing results on ARCESS data for Kola events.

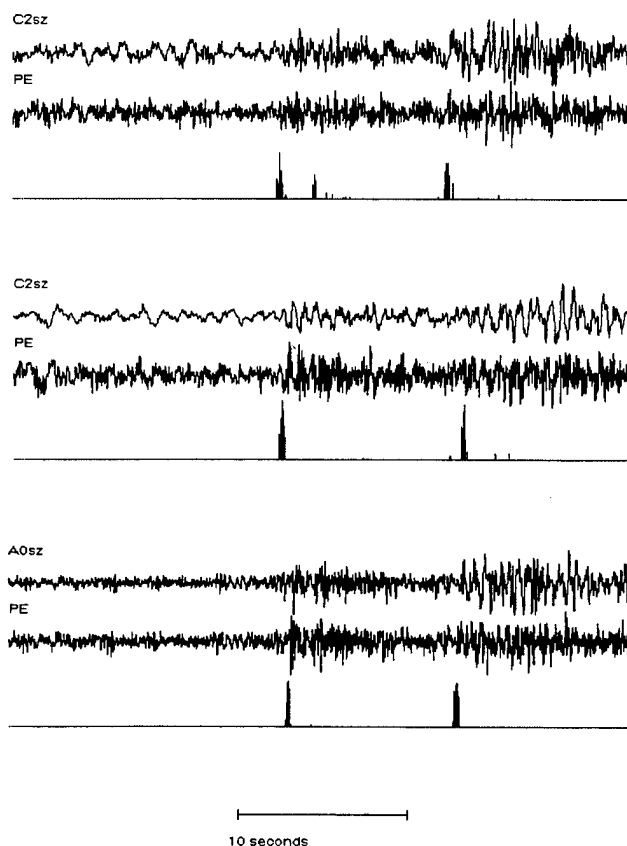


Figure 38. Very tight arrival time pick clusters were obtained using repeated applications of simulated annealing. These are processing results on ARCESS data for Kola events. Time length 102.4 seconds.

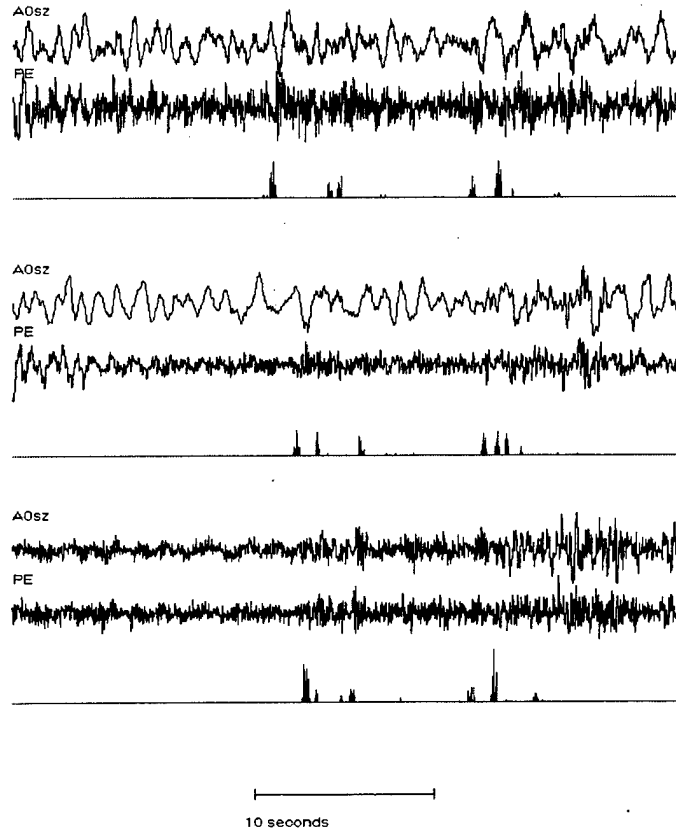


Figure 39. Some noisy regional events have multiple, ambiguous starts for the main arrival groups. This is reflected in the SA results which form multiple clusters. It must be noted, however, that a human analyst would also have difficulty in picking onset times in such cases. The Sn and Lg groups in this example have several energetic portions rather than a simple, impulsive start. Time length 102.4 seconds.

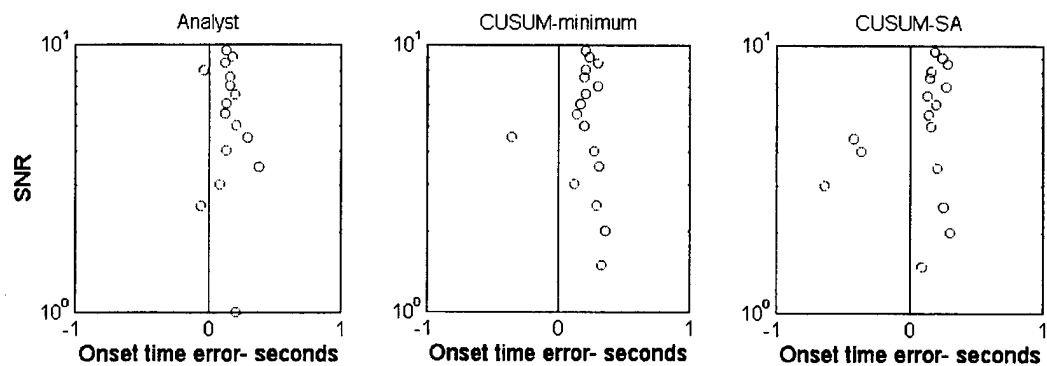
Evaluation of the Performance of the CUSUM Procedure for Estimating Pn Onset Times.

In the following we evaluate the performance of the combined CUSUM-SA procedure for picking onset times of first-arriving Pn phases. The evaluation is based on comparing the performance of human analysts to a) picking the absolute minimum of CUSUM formed around the first arrival b) picking the median of multiple picks using SA on the CUSUM. Prefiltering preceded all the data processing. The two kinds of prefilters applied to the seismograms were 2-7 Hz Butterworth band-pass filters and filters designed by taking the S/N^2 spectral ratio such that the maximum was set at unity and cutoffs were placed at the values at 0.24. The latter are similar to the filters that define "useful bandwidth". We have seen little difference in the performance of these filters in accordance with the comments made by *Kvaerna (1996)*. The events used had originally very high S/N ratios, especially on the prefiltered traces. To provide a "true" onset time the practically noise-free original trace was picked by the analyst. In order to construct noisy data, we have fitted a 15-th order AR model to the noise prior to the signal arrival and this model was used to construct independent noise samples by filtering Gaussian white noise. We have verified that the resulting artificial noise samples had spectra very close to those of the actual noise and thus the order of AR process was appropriate. The S/N ratio was defined as $SNR = \max(\text{signal amplitude}) / (\text{Twice the std. deviation of noise})$. This value is comparable to the SNR definition of *Kvaerna* who used a $\max(\text{signal}) / \max(\text{noise})$ ratio with short noise samples of a few hundred points, and we expect that the differences between these two definitions are inconsequential. Actually, our simulated records may be noisier for the same SNR value as *Kvaerna's*, since 5% of the points in a record must exceed two standard deviations so that the maximum in the noise sample will be larger than that value. The procedures described here were implemented in MATLAB which provides a convenient environment for quick prototyping at the expense of longer running times of the MATLAB interpreter. Practical software implementations of this methodology would require the use of the C codes that we have also developed independently, or the compilation of the MATLAB code (using the recently introduced MATLAB compiler).

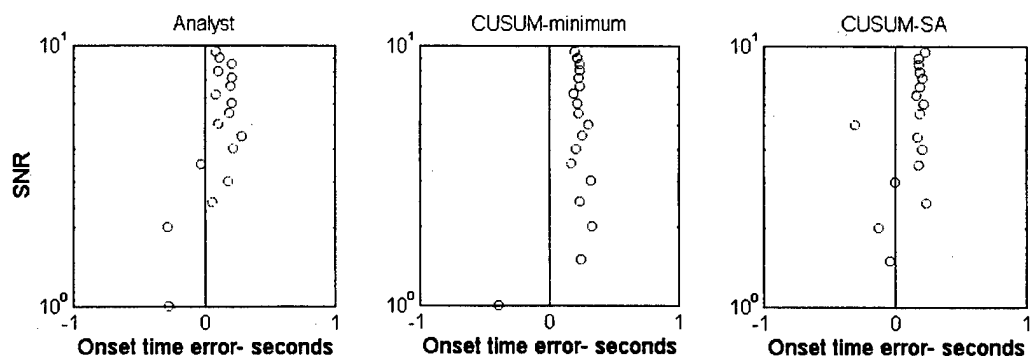
The process goes through a set of SNR values in increasing order starting with the worst value which is 0.5 and increasing to 9. In order to prevent the analyst from locking into the arrival time by comparing seismograms with varying SNR and by being able to 'peek through' low noise sections, we delayed the signal by random amounts before presenting each simulation.

The simulated noisy seismograms were presented to the analysts who were asked to click on their best estimates of onset. **Figure 38** shows some examples of these. Note that the visible spectral differences between signals and noise became small, especially at low to moderate SNR values. Following this the CUSUM was computed and the times were picked automatically. Finally, the noise-free trace is presented to the analysts for their best onset pick that was used as 'true' onset time. The differences between this value and the other onset time estimates were plotted for all the three methods against the logarithms of SNR values, with the random time shifts corrected for, of course. This is the same kind of evaluation method as the one used by *Kvaerna (1996a,b) and Yokota et al (1981)*.

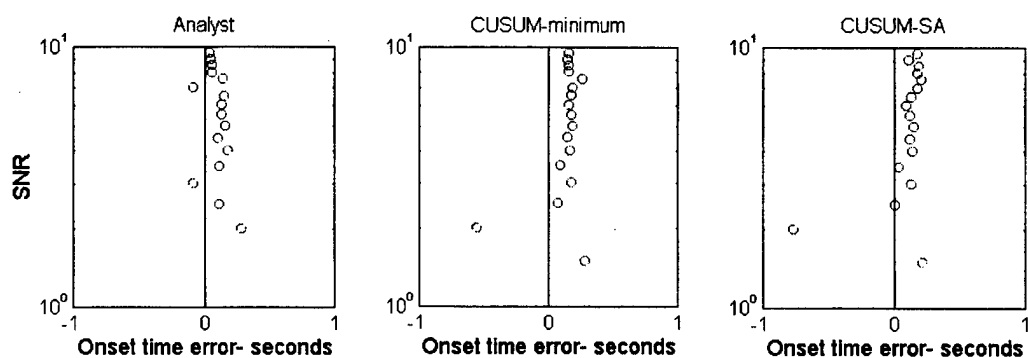
As the process starts at low S/N there are, naturally, some complete failures in picking the arrival time. We advised the analysts to click close to the ends of seismograms if they decided that it is not possible to see the signal. This resulted in error estimates larger than 2 sec, which we defined as failures. The failures of automatic processing results that followed were defined similarly ($\Delta t > 2$ sec). The reader may redefine the failures differently by setting this tolerance to a lower level he or she prefers.



K2054

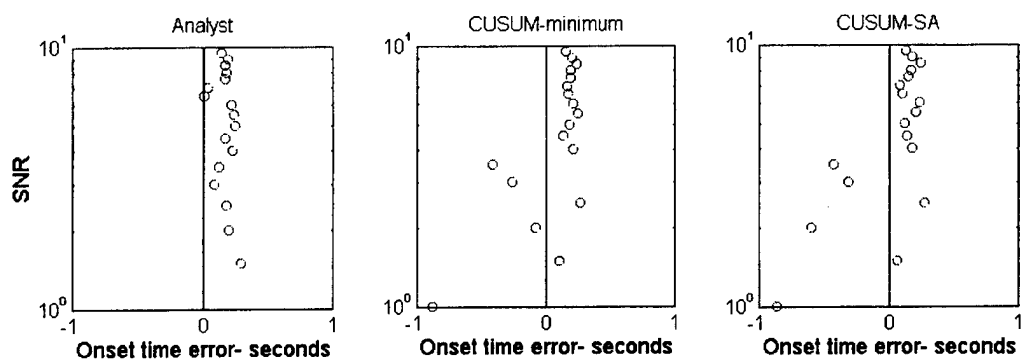


K2066

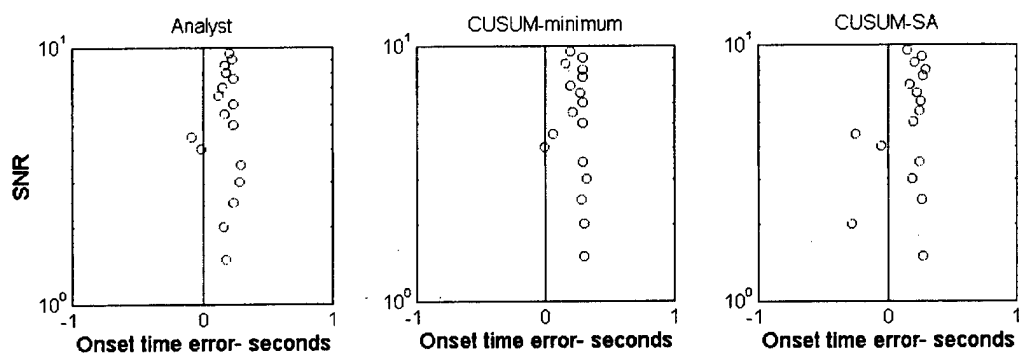


K2110

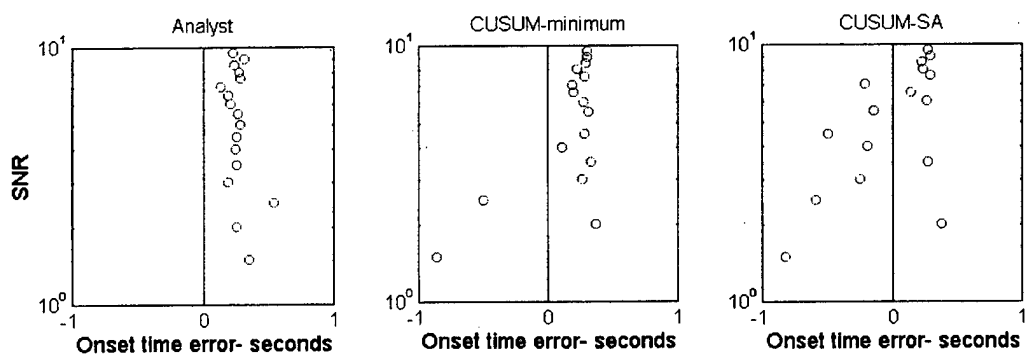
Figure 40.



K2147

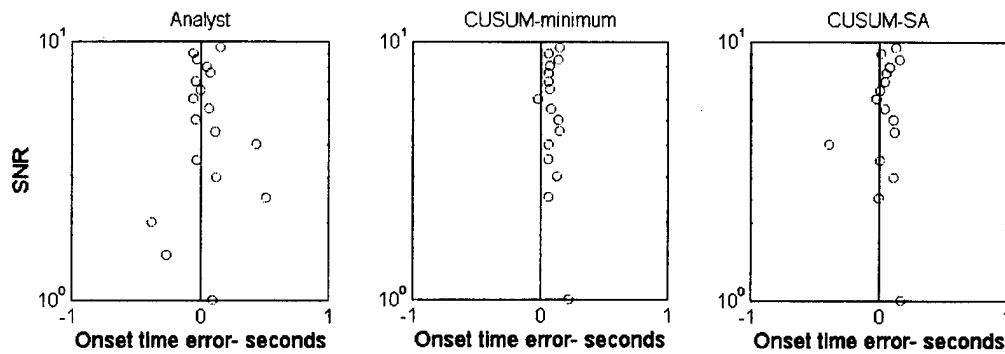


K2182

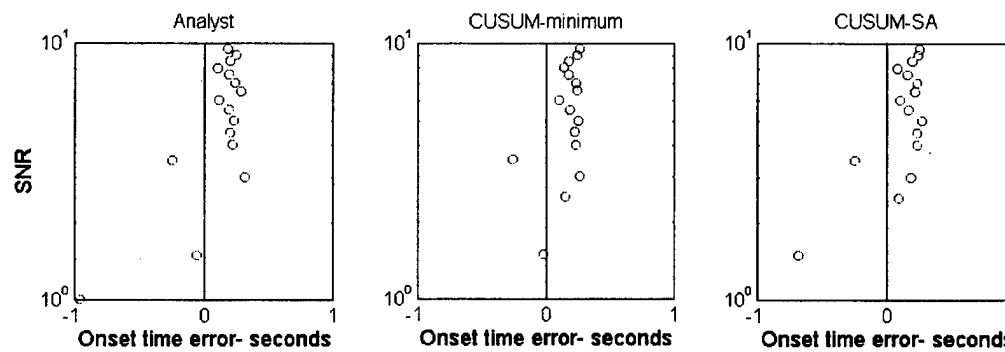


K2182

Figure 40.



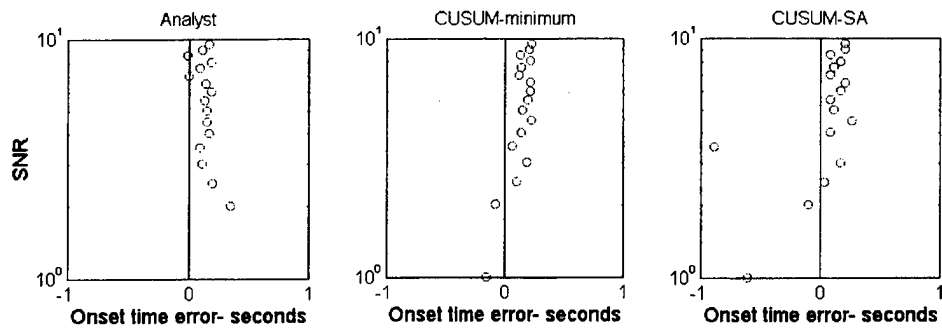
K4146



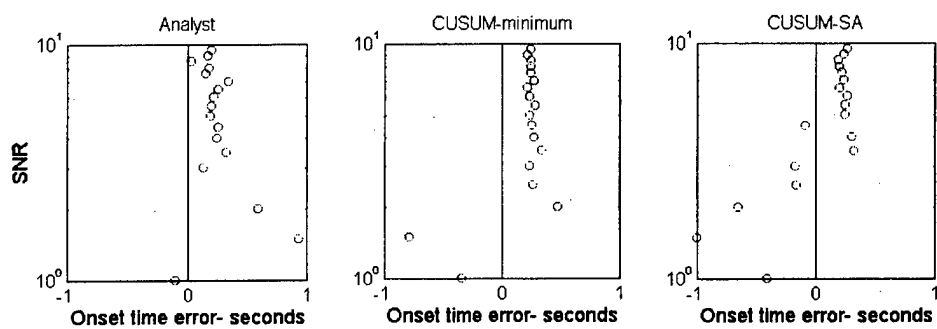
K4178

Figure 40. Onset time errors with simple 3-14 Hz bandpass prefiltering.

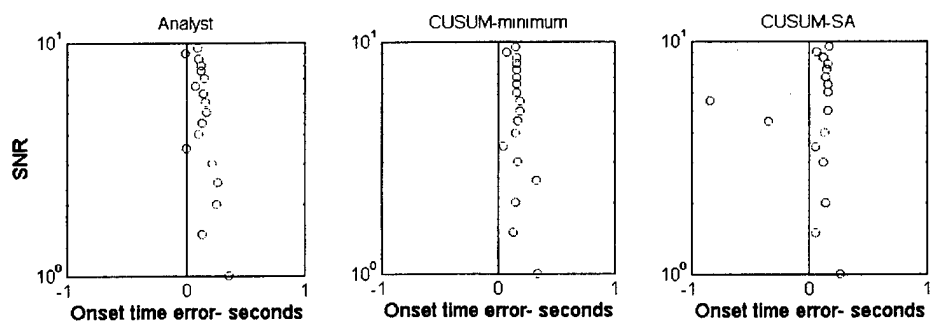
The procedures were repeated with S/N^2 filtering instead of fixed band pass filtering with onset time errors of similar accuracy as seen in the panels in **Figure 41**. Apparently, the kind of prefiltering, as long as it is reasonable, does not make much difference.



K2054sn

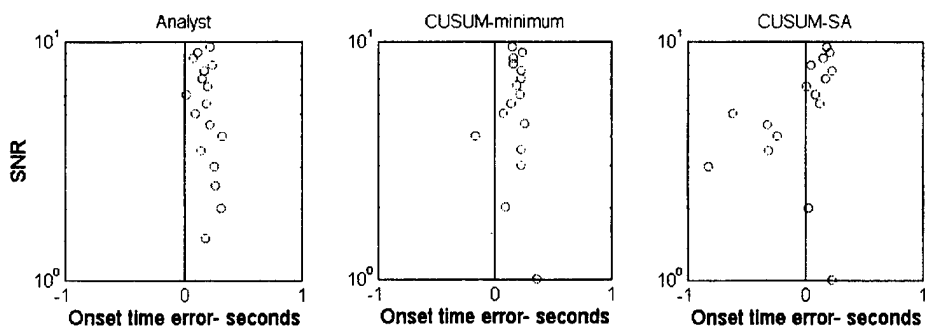


K2066sn

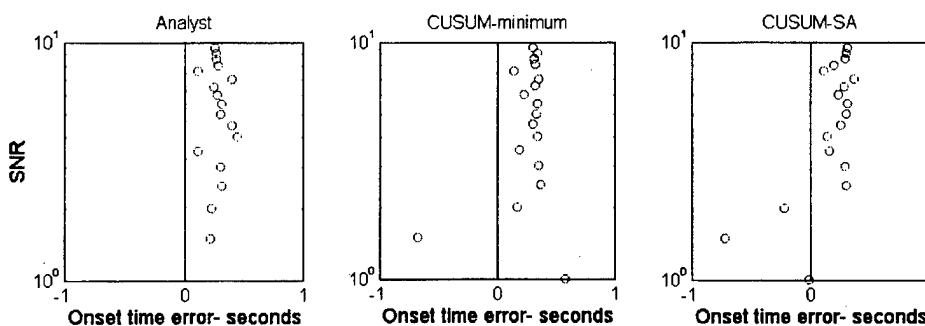


K2110sn

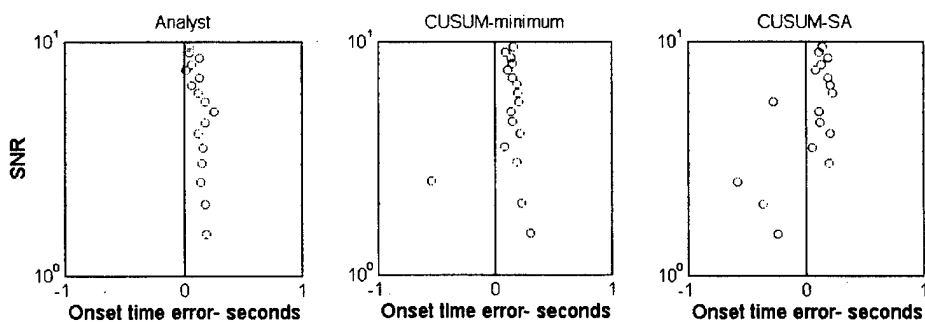
Figure 41.



K2147sn



K2182sn



K2246sn

Figure 41. Onset time errors the three procedures with S/N^2 filtering.

The surprising finding of these tests is that most automatic onset times at SNR levels above two were comparable in quality to that of the analyst. This is a lower level than the SNR of 5 quoted by Kvaerna for the current versions of the AR processor at IDC. The reasons for this difference are not obvious. It appears that while the AR method is sensitive to both RMS amplitude and spectral content changes, for the appropriately prefiltered seismograms the process is primarily driven by changes in the RMS amplitude level. Spectral differences between the noise and signal windows become minor after such prefiltering. Assuming that this is so, it seems to be computationally wasteful to compare the RMS fits to two not-too-different AR models, i.e. spectral contents, with the associated instabilities in computations, instead of simply comparing changes in the RMS amplitude levels which is much simpler. The other difference is that we have given up trying to find the precise point at which the change occurs between the two AR models. Rather, we try to find regions where the amplitude increases occur, and accept the ambiguities associated with such determination. The process will have to be reevaluated against improved versions of the AR processors at IDC currently under development.

Application of the CUSUM-SA Method to Segment Complete Regional Seismograms.

In the previous examples, we applied the CUSUM based onset time picker to the Pn-Pg and Sn-Lg arrival pairs separately. Since the amplitudes of the seismic trace are much larger for the last two it is difficult to subtract a single linear trend such that all four arrivals coincide with minima of the resulting function. Instead of subtracting a single linear trend one can use other ways to accomplish this. In our examples below we have subtracted a two-piece linear trend with a breakpoint between Pg and Sn. Other, equally effective, possibilities include the subtraction of a quadratic curve or some long-term average.

The basic assumption for the application of such methodologies is that we already have detected the event (by STA/LTA) and know the approximate times of the main arrivals (from slowness and polarization analyses such as those used in IMS or the generalized versions of them as described by *Der et al 1993*. Thus, we can position the breakpoint in the trend between Pg and Sn.

As we have indicated above, the various cluster analysis methods can be combined with repeated applications of SA to provide estimates to both the onset times and their uncertainties.

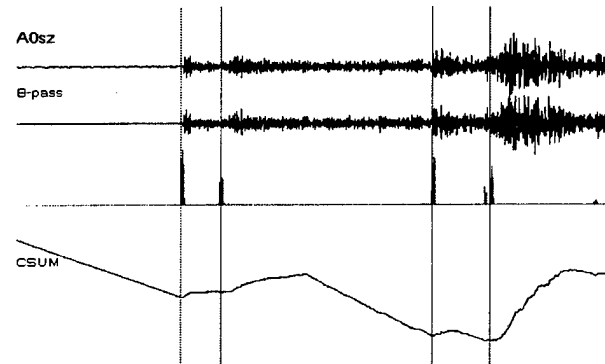
We have applied the K-means clustering algorithm to the populations of independent onset time estimations from SA (*Tou and Gonzalez 1974*). This is really not the best method to do this task, but since we already had a working program for the K-means algorithm it was expedient to use it. The 1-D version of K-means was modified by squaring the distance measure, which would be otherwise just the linear distance between points. This enhanced the property of the algorithm to identify the tight clusters of onset times, instead of merging several distinct clusters into one. When the K-means algorithm was used it was found that the best way to apply this method of cluster analysis was to specify a larger number of clusters than the number of expected arrivals and discard the clusters with membership less than 10% of the total onset time estimates. This approach eliminated the few scattered values and concentrated on the few (typically four) main arrival clusters within the search window.

Once the cluster centers are identified (K-means supplies these), some adjustment for the late bias of the cluster center can be accomplished by moving the estimated onset time by 1.5-2 standard deviations (of the cluster) to earlier times. This strategy is sufficient for removing visible bias due to the shifts in minima caused by the imposition of linear trend and thus put the onset time to where a human analyst would pick it. Since onset times of secondary arrivals are generally poorly defined, the algorithm performs not worse than a human analyst. The picking of Pn onset times is a separate issue requiring a smaller time window.

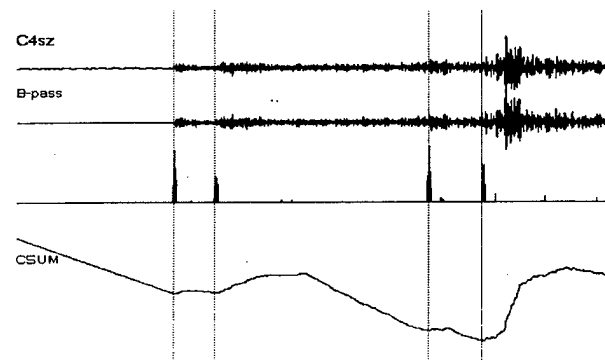
Figures 42 to 44 show examples of the onset time determinations by the automatic algorithm described above as applied to the events analyzed by *Der et al 1993*. In **Figure 42**, we plot all the main functions, the raw trace, the 4-10 Hz band-pass filtered trace, the histograms of the SA onset time picks and the cumulative sum (CUSUM) of the absolute amplitudes of the band-pass filtered trace. The final onset time picks are the vertical thin lines. The figure shows the results for a set of K2 mine events. Since these events have very clear phase beginnings and occurred at the same quarry, the phases were picked fairly consistently from event to event, i.e. the spacings of the various automatically identified arrivals are very close. Only one Sn and one Pg phase was missed.

Similarly good results were obtained for some other mines (**Figure 43**). We have found that in many cases where there were only three main visible arrivals the algorithm adjusted to this situation automatically.

On the other hand, some results were not as good, especially some K4 mine events. The waveforms of these events have numerous amplitude fluctuations and the initial P phases have emergent beginnings. The K-means algorithm often groups scattered picks into arbitrary groups and the emergent beginnings are missed. As we have pointed out above some of these problems could be eliminated by the substitution of some other cluster identification algorithm in place of K-means.



K2054

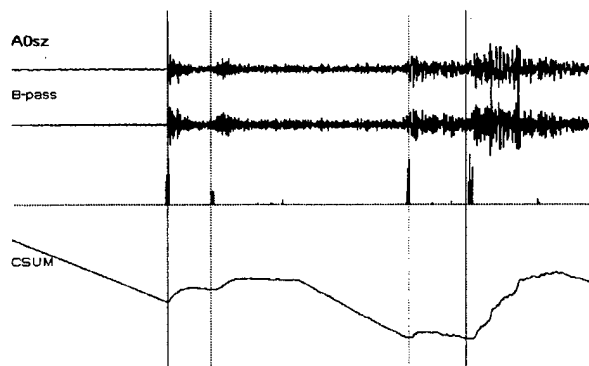


K2066

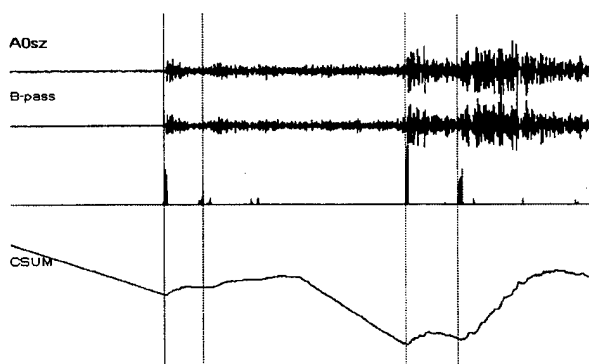


K2110

Figure 42.



K2147

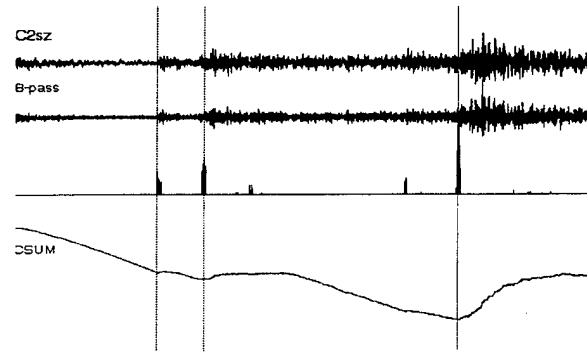


K2182

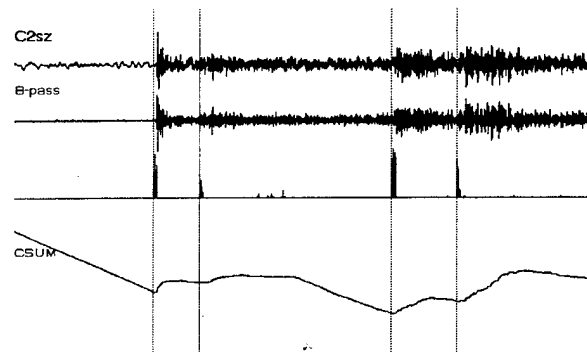


K2219

Figure 42.



K2246

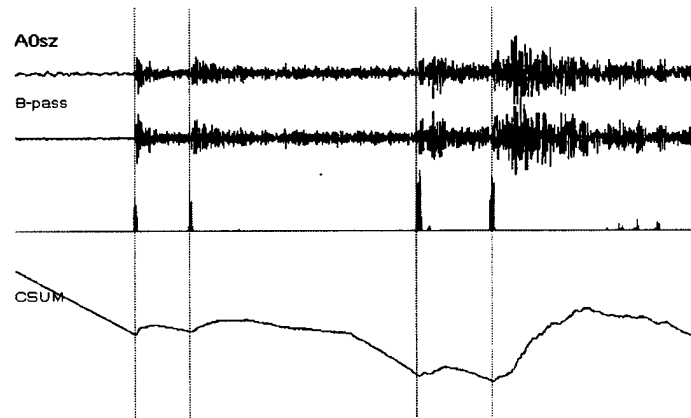


K2282

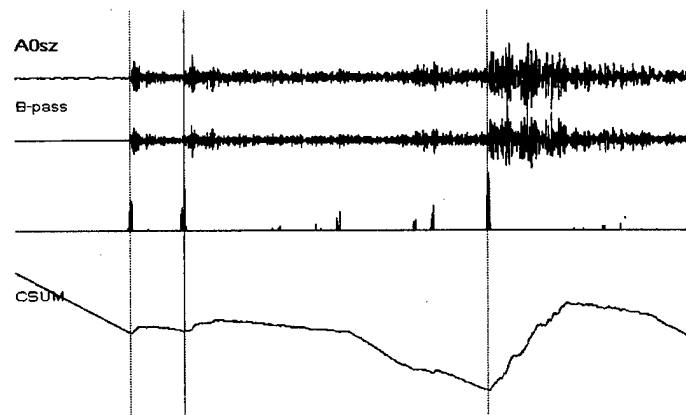


K2285

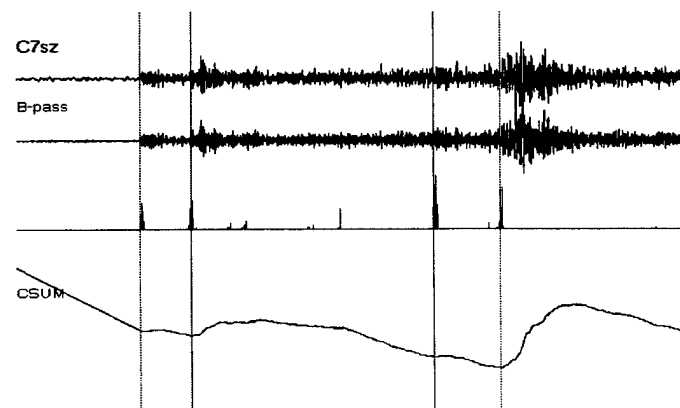
Figure 42. These are the results for the set of K2 events analyzed by Der et al (1993). Since these have well-defined phases with abrupt beginnings, all were picked with the exception of one (weak) Sn and a Pn. The relative times of the picks are also consistent. Time lengths are 102.4 seconds.



K5089

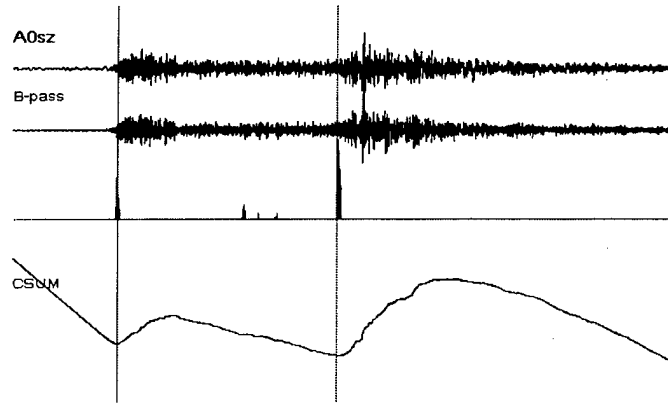


K5125

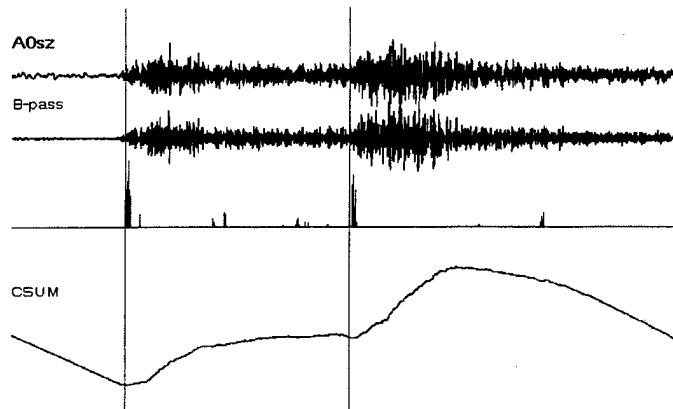


K5222

Figure 43.

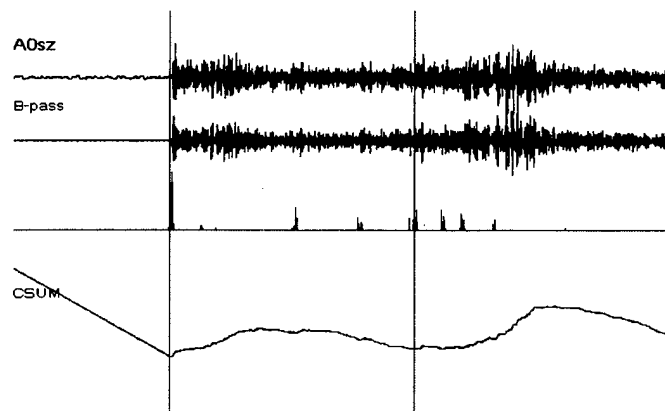


K8223

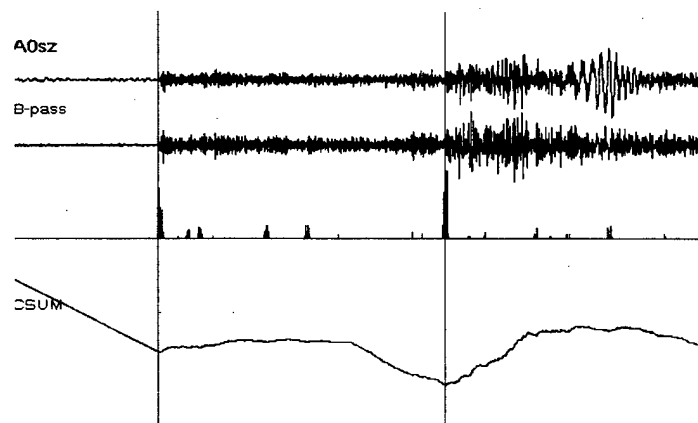


K8279

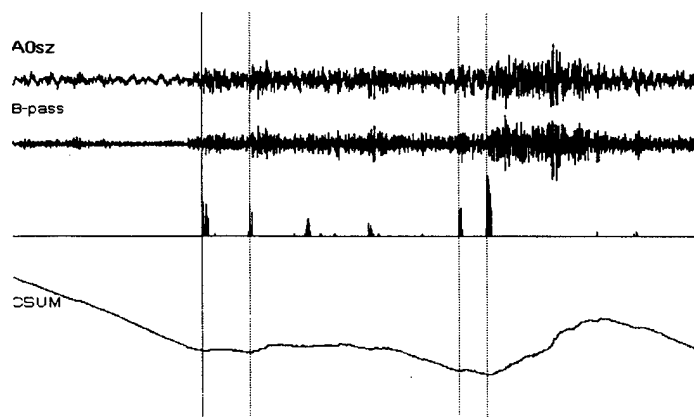
Figure 43. These are results for three K5 mine events and two K8 mine events. Time lengths are 102.4 seconds. Although some Pn times are late, such errors can be corrected by using separate procedures for Pn first arrivals as shown above.



K4178

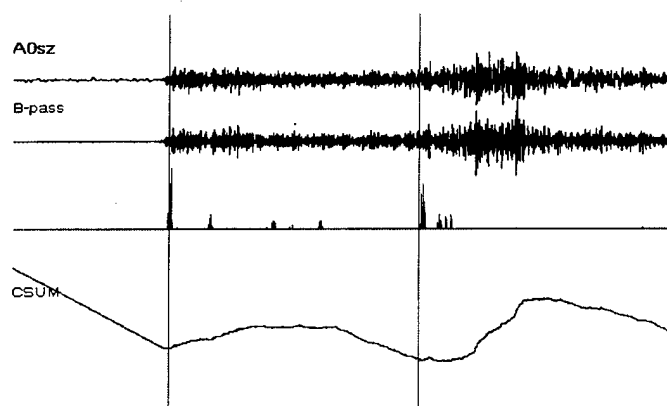


K4230



K4270

Figure 44.



K4272

Figure 44. These examples from the K4 group illustrate cases where we still had problems. These include missing weak phases, missing emergent phases, late picks missing emergent beginnings and having double picks at times where an analyst would not pick anything. Most of these problems appear to be associated with the K-means grouping which will be eliminated in the future. The main problems with automatic onset time picking seemed to be associated with the K-means algorithm which could be eliminated in the future and some more robust method substituted for it. Although it seemed to work well for events sets with a few well-defined arrivals, some problems were encountered for events where the amplitudes fluctuated, creating many small clusters. In some cases sets of small clusters were grouped into one by the K-means algorithm, thus creating an arrival that would not be seen by an analyst as such. We see these problems as due to the K-means method and not to the basic approach. The K-means algorithm will be substituted by a cluster finder that progresses with time and is combined with some algorithms that limit the cluster size, spread and automatically eliminates outliers.

In these tests we have paid no attention to computational efficiency; the main goal was to demonstrate the feasibility of computer onset time estimation. The process with 300 individually estimated onset times and K-means sorting, which takes two seconds on a 166MHz Pentium with compiled FORTAN code, can be speeded up considerably by the means described next. First of all, the starting points for SA searches could be moved closer to the known approximate onset times, instead of being distributed randomly as above and the initial 'temperature' could be lowered and fewer cooling steps could be taken. The cooling sequence could be optimized also. These steps could easily reduce the amount of random searching by factors of two to three. The added benefit for K-means would be that the input could be sorted into fewer clusters since there would be fewer scattered onset times. The independent SA searches can also be parallelized on suitable computers, thus reducing the time to a fraction of it. Instead of 1-D K-means, more efficient and simpler methods can be used for identifying the main clusters. It is certain that the processes tested described above are needlessly computer-intensive and complex and thus could be simplified considerably.

Regardless of the complexity of the algorithms tested, even a two-second running time would be no obstacle to using the algorithms unmodified, since the process can always be run in the background, while the analyst is busy with other tasks, and in the fully automatic mode a two-second running time is sufficiently fast for processing all events in real time.

Multichannel Deconvolution

With regards to the multichannel deconvolution method, we attempted to modify it in order to make more useful for isolated teleseismic events as opposed to events clustered at test sites. The main purpose is to reduce site-source tradeoffs in analyzing the data (*Der et al 1986, 1987, 1992*). The latter scenario is more appropriate to isolated violations of a test ban treaty and to discrimination of nuclear explosions from earthquakes on a global basis. Applying the concepts of our multichannel deconvolution to such events as seen at smaller arrays and/or networks requires some revision of the procedures applied. Since there are no multiple events in the same source area, the site spectral factors cannot be improved by event-averaging. Sites in a network with the strongest site distortion (non-transparent sites) must be identified and eliminated when estimating the source factors.

On the other hand, closely grouped sites, such as those at small regional arrays, will have similar site effects that may influence the source estimates. Obviously, we are interested in the sources and not in the site effects. The remedy we recommend is to test the teleseismic P waveforms for clustering using the K-means algorithm. In a large network the cluster analysis will identify outlier stations (non-transparent stations). If, on the other hand, the waveforms cluster according to their geographical proximity (such that the waveforms from each regional array would form a cluster), then one should use only a few waveforms from each such array to avoid contamination from site effects. We have written a program to perform K-means cluster analysis.

Multichannel deconvolution for the single event case boils down to something resembling the "phaseless seismogram" method developed by *Stewart and Douglas 1983*. During the reporting period, we have implemented the phaseless seismogram as an option that can be used for single events.

CONCLUSIONS AND RECOMMENDATIONS

In this report an adaptive approach for automatic identification of regional arrivals is tested. The work was aimed at developing regional phase identification and detection techniques suitable to small regional arrays with much fewer sensors than those present at NORESS, ARCESS or GERESS.

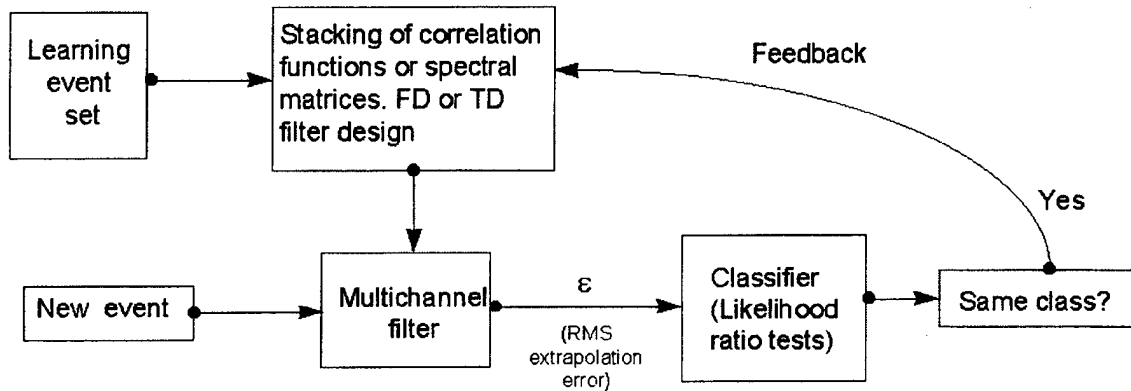


Figure 45. A general adaptation scheme for recognizing regional events.

The general approach is to collect array data for a set of training events (learning set) known to be close to each other and compute a set of digital filters that extrapolate the motion at one sensor from that at the other sensors for each regional arrival. The success of this extrapolation, for all arrivals simultaneously, is a criterion for the assignment of other events to the same location (**Figure 45**). This approach apparently works for the Kola peninsula data set we have tested. The method can be made fully automatic for small arrays of the type that will be used in global monitoring. Despite these results, the methodology must be tested using more difficult cases.

Extensive testing of the original frequency domain formulation presented by *Der et al (1993)* was done. From the work done thus far we conclude that it works better in regional arrival discrimination than the conventional method based on 3-component rectilinearity and slowness. The technique works well for ARCESS recordings of the K2 and K4 mines in the Kola for which 9 and 11 events were available respectively. In these tests we have used only six sensors, a three component combination at A0 and three vertical sensors from the C ring. We have also

tested the leave-one-out method for both arrays for the same combination. These tests showed that the method is very robust for Pn and Pg, but one outright failure of picking Lg occurred for the K2 mine and some of the correlations were significantly lower for Sn and Lg. This indicates that the method will not work well if the number of training events is much below eight or nine.

For the frequency domain case we have also formulated a testing methodology based on the F statistic. This method for testing has not been implemented yet, as the work in this paper used the normalized correlation coefficients in *Der et al (1993)*.

Fully automatic processing of regional seismograms appears to be quite feasible. After event detection by conventional means (STA/LTA), conventional or generalized polarization analyses (*Der et al 1993*) can be used for locating the main wave groups in the regional seismograms. In the case where no suites of collocated master events are available, these can be furnished by standard slowness-rectilinearity analyses.

CUSUM based algorithms can be used effectively for determining the onset of Pn with an accuracy comparable to a human analyst. Late bias for emergent, noisy arrivals is unavoidable and common to both the human analysts and any automatic process and thus not the sole property of automatic algorithms (*Kvaerna 1995*).

The onset times of secondary phases (Pg, Sn and Lg) can be determined, somewhat less accurately, by CUSUM based searches using cluster analysis on suites of picks generated by using repeated applications of simulated annealing. The algorithms tested in this report can be considerably simplified in the future.

Full automatic analysis of regional seismograms can be accomplished in real time with moderate amount of computer power (on the 486 or Pentium PC level). S/N limitations are common to all processes.

Onset time estimates from frequency prefiltering combined with various forms of amplitude related CUSUM based algorithms give results that compare favorably with those produced by human analysts and the AR model based onset time algorithms.

The exact nature of the prefilter for enhancing the SNR contrast between the arrivals and the background noise, fixed band-pass, AR or the more exact S/N^2 , does not seem to be critical as long as they are reasonably close to the last of these. Various parts of this report used all three of these prefiltering methods.

As revealed by examining regional signals with high S/N ratios, many of them build up gradually and have emergent beginnings. Consequently, late bias of onset times for noisy regional signals is common to all automatic methods and the analyst determinations as well.

Although the method of picking the minimum of the CUSUM combined with a linear trend gives fairly accurate onset times, it seems to be more advantageous to utilize simulated annealing (SA) for repetitively finding the minima. This approach gives populations of multiple onset times that can be further processed by identifying the largest clusters of these as arrivals and derive measures of their statistical uncertainties. More work is needed to define the best non-parametric statistical approaches to do this.

The CUSUM based methods are especially suited for picking onset times of later arrivals in the regional seismograms. Since the spectral content of a regional seismogram changes little as the time progresses, onset time estimation must be mostly based on amplitude changes, not spectral changes as in the AR model based methods.

CUSUM-based methods to pick phase onset times can also be developed based on statistics that are diagnostic of polarization, slowness, and spectral changes.

REFERENCES

- Basseville, M. and I.V. Nikiforov (1993), *Detection of Abrupt Changes: Theory and Application*. Prentice Hall Information and System Science Series, Prentice Hall, Englewood Cliffs, NJ.
- Baumgardt, D.R., and K.A. Ziegler (1988), Spectral evidence of source multiplicity in explosions; application to regional discrimination of earthquakes and explosions. *Bull. Seism. Soc. Am.*, 80, Part B, 1874-1892.
- Christoffersson, A., and Roberts, R. (1996), Trinity or verity? In "Monitoring a Comprehensive Test Ban Treaty." E.S. Husebye and A. M. Dainty Editors. Nato ASI Series, Kluwer Academic Publishers.
- Der, Z.A., Hirano, M.R., and R.H. Shumway (1990), Coherent processing of regional signals at small seismic arrays. *Bull. Seism. Soc. Am.*, 80B, 2161-2176.
- Der, Z.A., Baumgardt, D.R., and R.H. Shumway (1993), The nature of particle motion in regional seismograms and its utilization for phase identification. *Geophys. J. Int.*, 115, 1012-1024.
- Der, Z.A., Baumgardt, D.R. and R.H. Shumway (1993), The nature of particle motion in regional seismograms and its utilization for phase identification. *Geophys. J. Int.*, 115, 1012-1024.
- Der, Z.A. (1994), Genetic algorithm (GA) machine learning of seismic waveform characteristics. SBIR Phase II Final Report. Prepared for the Advanced Research Project Agency. ENSCO Inc. Springfield, VA.
- Der, Z.A., Lees, A.C., Shumway, R.H., McElfresh, T.W. and M.E. Marshall (1986), Multichannel deconvolution of P waves at seismic arrays and three component stations. TGAL-86-6, Teledyne-Geotech, Alexandria, VA.

Der, Z.A., Shumway, R.H. and Lees, A.C. (1987), Multichannel deconvolution of P waves at seismic arrays. *Bull. Seism. Soc. Am.*, **77**, 195-211.

Der, Z.A., Lees, A.C., McLaughlin, K.L. and R.H. Shumway (1992), Deconvolution of short period teleseismic and regional time series. In "*Statistics in the Environmental and Earth Sciences*", A.T. Walden and P. Guttorp Editors, Edward Arnold, New York-Toronto.

Douglas, A., Bowers, D., and Young, J.B. (1997), On the onset of P seismograms. *Geophys. J. Int.*, **129**, 681-690.

Helstrom, C.W. (1995), *Elements of Signal Detection and Estimation*, Prentice Hall, Englewood Cliffs, NJ.

Jurkevics, A. (1988), Polarization analysis of three-component array data. *Bull. Seism. Soc. Am.*, **78**, 1725-1743.

Kvaerna, T. and F. Ringdal (1992), Integrated array and three-component processing using a seismic microarray. *Bull. Seism. Soc. Am.*, **82**, 1725-1743.

Kvaerna, T. (1995), Automatic onset time estimation based on autoregressive processing. Semiannual Technical Summary, 1 April-30 September 1995. NORSAR, Sci. Report No. 1-95/96, Kjeller, Norway.

Kvaerna, T. (1996a), Quality assessment of automatic onset times estimated by the autoregressive method. Semiannual Technical Summary, 1 April-30 September 1995. NORSAR, Sci. Report No. 1-95/96, Kjeller, Norway.

Kvaerna, T. (1996b), Time shifts of phase onsets caused by SNR variations, Semiannual Technical Summary, 1 October 1995-31 March 1996. NORSAR, Sci. Report No. 2-95/96, Kjeller, Norway.

Maeda, N. (1985), A method for reading and checking phase time in auto-processing system of seismic wave data (in Japanese with English abstract), *J. Seismol. Soc. Jpn.*, **38**, 365-379.

Mykkeltveit, S. (1992), Mining explosions in the Khibiny Massif (Kola Peninsula in Russia) recorded at the Apatity three-component station. PL-TR-92-2253 , ADA 266065.

Nikiforov, L.V. and Tikhonov, I. N. (1986), Application of change detection theory to seismic signal processing. In "Detection of Abrupt Changes in Signals and Dynamical Systems "M. Basseville and A. Benveniste Editors. Lecture Notes in Control and Information Sciences, LNCIS 77, Springer, New York.

Nikiforov, L.V., Tikhonov, I.N., and Mikhailova, T.G. (1989), Automatic on-line processing of seismic data- Theory and applications. Far Eastern Dept. of USSR Academy of Sciences, Vladivostok, USSR (In Russian).

Press, W.H., Flannery, B.P., Teukolsky, S.A. and W.T. Vetterling (1986), *Numerical Recipes: The Art of Scientific Computing*. Cambridge University Press.

Shumway, R.H. (1989), *Applied Statistical Time Series Analysis*. Prentice Hall.

Stewart, R.C. and Douglas, A. (1983), Seismograms for phaseless seismographs. *Geophys. J. Roy. Astr. Soc.*, **72**, 123-152.

Suteau-Henson, A. (1991), Three-component analysis of regional phases at NORESS and ARCESS: polarization and phase identification. *Bull. Seism. Soc. Am.*, **81**, 2419-2440.

Takanami, T. (1991), A study of detection and extraction methods for earthquake waves by autoregressive models. *J. Fac. Sci. Hokkaido, U.*, Ser VII, 9, 67-196.

Tarvainen, M. (1991), Detecting local and regional seismic events using the data adaptive method at the VAF seismograph station in Finland. *Bull. Seism. Soc. Am.*, **81**, 1372-1379.

Tou, J. T. and Gonzalez (1974), *Pattern Recognition Principles*, Addison-Wesley.

Vogfjord, K. S., and Langston, C. A. (1990), Analysis of regional events recorded at NORESS. Bull. Seism. Soc. Am., 80, 2016-2031.

Wiggins, R. and E.A. Robinson (1975), An iterative implementation of the multichannel filtering problem, J. Geophys. Res., 70, 1885-1891.

Yokota, T., Zhou, S., Mizoue, M., and Nakamura, I. (1981), An automatic measurement of arrival time of seismic waves and its application to an on-line processing system (in Japanese with English abstract), Bull. Earthquake. Res. Inst. Univ. Tokyo, 55, 449-484.